OPTIMIZATION OF NICKEL, COBALT AND LITHIUM RECOVERY PROCESSES FROM SPENT LI-ION BATTERIES

A THESIS SUBMITTED TO
THE GRADUATE SCHOOL OF NATURAL AND APPLIED SCIENCES
OF
MIDDLE EAST TECHNICAL UNIVERSITY

BY

FIRAT TEKMANLI

IN PARTIAL FULFILLMENT OF THE REQUIREMENTS
FOR
THE DEGREE OF MASTER OF SCIENCE
IN
METALLURGICAL AND MATERIALS ENGINEERING

DECEMBER 2022

Approval of the thesis:

OPTIMIZATION OF NICKEL, COBALT AND LITHIUM RECOVERY PROCESSES FROM SPENT LI-ION BATTERIES

submitted by **FIRAT TEKMANLI** in partial fulfillment of the requirements for the degree of **Master of Science** i**n Metallurgical and Materials Engineering, Middle East Technical University** by,

Prof. Dr. Halil Kalıpçılar
Dean, Graduate School of **Natural and Applied Sciences** _____

Prof. Dr. Ali Kalkanlı
Head of the Department, **Metallurgical and Materials Eng., METU** _____

Prof. Dr. M. Kadri Aydınol
Supervisor, **Metallurgical and Materials Eng., METU** _____

Examining Committee Members:

Prof. Dr. Caner Durucan
Metallurgical and Materials Eng, METU _____

Prof. Dr. M. Kadri Aydınol
Metallurgical and Materials Eng, METU _____

Prof. Dr. Tayfur Öztürk
Metallurgical and Materials Eng, METU _____

Assist. Prof. Dr. Çiğdem Toparlı
Metallurgical and Materials Eng, METU _____

Assoc. Prof. Dr. Göknur Büke
Material Science and Nanotechnology Eng, TOBB ETU _____

Date: ...

I hereby declare that all information in this document has been obtained and presented in accordance with academic rules and ethical conduct. I also declare that, as required by these rules and conduct, I have fully cited and referenced all material and results that are not original to this work.

Name Last name :

Signature :

ABSTRACT

OPTIMIZATION OF NICKEL, COBALT AND LITHIUM RECOVERY PROCESSES FROM SPENT LI-ION BATTERIES

Tekmanlı, Fırat
Master of Science, Metallurgical and Materials Engineering
Supervisor : Prof. Dr. M. Kadri Aydınol

December 2022, 57 pages

Since lithium-ion batteries are standard in electric vehicles and electrical devices and have the potential to be used widely in the future, it is essential to recycle end-of-life batteries. Waste lithium-ion batteries are harmful to the environment and human health and should be recycled also due to their critical metals. Lithium-ion batteries can be classified according to their cathode chemistry. In this thesis, the recycling of lithium-ion batteries with NMC-type (Nickel- Manganese-Cobalt) cathode chemistry was discussed. Two different approaches have been studied for the recycling of waste batteries. The first approach concerns the use of cathode active materials to make new electrodes by stripping them from the current collector foil and directly turning them into sludge. Three different methods have been studied for this approach. These are pyrolysis method, dissolution of PVDF method and dissolving of aluminum foil method. The pyrolysis method shows negative contribution on the performance of cathode active materials in terms of both capacity and cycle life. The dissolution of PVDF method shows promising electrochemical results but the residual PVDF leads to particle agglomeration which is not desired.

In the dissolution of aluminum method, residual aluminum leads poor capacity retention. The other approach is to leach waste lithium ion cathodes with acid and then synthesize new cathode active material by direct co-precipitation method with the obtained leaching solution. In this approach, up to 99% Li, 97% Ni, 96% Co and 98% Mn by weight are recovered from the cathode mass and new cathode active materials were synthesized via co-precipitation method. The electrode prepared with this material shows 94.2% capacity retention after 50 cycle and discharge capacities at first and final were 151.58 mAh/g and 142.83 mAh/g,respectively, at 0.5C rate with the reference capacity of NMC-111 is 155 mAh/g.

In both approaches, the aim is to create a closed-loop recycling process and to eliminate the extra steps as in conventional methods.

Many pyrometallurgical and hydrometallurgical studies have been carried out worldwide for recycling processes. Still, it is not a closed-loop process yet, and hydrometallurgical studies with various acids and reducing agents need optimization. Lithium-ion batteries, intended to be recycled by hydrometallurgical methods, not by pyrometallurgical modes in terms of environmental pollution, are disassembled in this thesis. The emission of HF gas during the processes was investigated and its effect on the cathode properties was investigated. Acid leaching was carried out with various acids and reducing agents. Eventually, the closed-loop recycling and resynthesis processes successfully demonstrated the targeted performance.

Keywords: Recycling, Li-ion Battery, Leaching, Closed-Loop Recycling, Co-precipitation

ÖZ

ATIK Lİ-İYON BATARYA KATOTLARINDAN NİKEL, KOBALT VE LİTYUM GERİ KAZANIMI PROSESLERİNİN OPTİMİZASYONU

Tekmanlı, Fırat
Yüksek Lisans, Metalurji ve Malzeme Mühendisliği
Tez Yöneticisi: Prof. Dr. M. Kadri Aydınol

Aralık 2022, 57 sayfa

Lityum iyon piller elektrikli araçlarda ve elektrikli cihazlarda yaygınca kullanıldığından ve gelecekte yaygın olarak kullanılmaya devam etme potansiyeline sahip olduğundan, ömrünü tamamlamış pillerin geri dönüştürülmesi zorunluluktur. Atık lityum iyon piller çevreye ve insan sağlığına zararlıdır ve içerdiği kritik metaller nedeniyle de geri dönüştürülmelidir. Lityum iyon piller, katot kimyalarına göre sınıflandırılabilir. Bu tezde, lityum iyon pillerin NMC tipi (Nikel-Mangan-Kobalt) katot kimyası ile geri dönüşümü tartışılmıştır. Atık pillerin geri dönüşümü için iki farklı yaklaşım incelenmiştir. İlk yaklaşım, akım toplayıcı folyodan (katot için genellikle alüminyum folyo) katot aktif malzemeyi sıyırmak ve bu tozları doğrudan çamura dönüştürerek yeni elektrotlar yapmak için kullanmakla ilgilidir. Bu yaklaşım için üç farklı yöntem incelenmiştir. Bunlar piroliz yöntemi, PVDF'nin çözünmesi yönteminin ve alüminyum folyonun çözündürülmesi yöntemidir. Isıl işlem yöntemi, katot aktif malzemelerin performansına hem kapasite hem de çevrim ömrü açısından olumsuz etki göstermektedir. PVDF çözünme yöntemi ise umut verici

elektrokimyasal sonuçlar göstermiştir, ancak kalıntı/çözünmemiş PVDF, istenmeyen partikül aglomerasyonuna yol açmaktadır.

Alüminyumun çözündürülmesi yönteminde, kalıntı alüminyum yetersiz kapasite korunumu problemine yol açmaktadır. Diğer yaklaşım, atık lityum iyon katotların asit ile liç edilmesi ve daha sonra elde edilen liç çözeltisi ile doğrudan birlikte çöktürme yöntemi ile yeni katot aktif materyalinin sentezlenmesidir. Bu yaklaşımda, katot kütlesinden %99'a kadar Li, %97Ni, %96 Co ve %98 Mn geri kazanılmış ve birlikte çöktürme yöntemi ile yeni katot aktif malzemeler sentezlenmiştir. Bu malzeme ile hazırlanan elektrot, 50 döngüden sonra %94,2 kapasite korunumu göstermektedir ve ilk ve son deşarj kapasiteleri sırasıyla 151.58 mAh/g ve 142.83 mAh/g olup, 0.5C hızında şarj/deşarj edilerek NMC-111'in referans kapasitesi 155 mAh/ g değerinde alınmıştır.

Her iki yaklaşımda da amaç, kapalı döngü bir geri dönüşüm süreci oluşturmak ve mevcut yöntemlerde olan kompleks proseslerin ve fazladan maliyet gerektiren konvansiyonel yöntemlerin dezavantajlarını ortadan kaldırmaktır.

Geri dönüşüm süreçleri için dünya çapında birçok pirometalurjik ve hidrometalurjik çalışma yapılmıştır. Yine de, henüz kapalı döngü bir proses değildir ve çeşitli asitler ve indirgeyici maddelerle yapılan hidrometalurjik çalışmaların optimizasyona ihtiyacı vardır. Çevre kirliliği açısından pirometalurjik metodlarla değil, hidrometalurjik yöntemlerle geri dönüştürülmesi amaçlanan lityum iyon piller bu tezde öncelikle deşarj edilerek komponentlerine ayrılmıştır. Çalışmada kullanılan atık lityum iyon pil katotlarında bağlayıcı olarak kullanılan organiğin PVDF olduğu belirlenmiştir. İşlemler sırasında HF gazı emisyonun ve katotun yapısınıa ve davranışına olan etkisi araştırılmıştır. Asit liçi, çeşitli asitler ve indirgeyici ajanlar ile çalışılmıştır.

Anahtar Kelimeler: Geri dönüşüm, Li-iyon Batarya, Liç, Kapalı devre geri dönüşüm, Eş-çöktürme

Dedicated to META Nickel Cobalt R&D Department

ACKNOWLEDGMENTS

I would like to express my endless thanks to my advisor, Kadri Aydınol, who provided all his help and support throughout this whole time. It is extremely valuable for me that he is by my side in my problems and guiding me through all his busywork.

Apart from that, I would like to thank my dear manager Nuray Demirel and all my friends in Meta Nickel Cobalt R&D department. I would like to express my sincere thanks to Şerif Kaya, who helped me the most during this thesis process, contributed so much to me that I cannot count, and conveyed to me his countless and invaluable knowledge and experience. Moreover, I would like to thank my friends in the Meta Nickel Cobalt laboratory team, as well as METU Metallurgical and Materials Engineering laboratory technician Nilüfer Özel. I sincerely thank Cansu Savaş Uygur and Kadir Özgün Köse, who have always helped me in our lithium-ion battery laboratory since the beginning.

Finally, I would like to thank all my friends.

TABLE OF CONTENTS

LIST OF TABLES

TABLES

LIST OF FIGURES

FIGURES

LIST OF ABBREVIATIONS

CRM: Critical Raw Materials

EEE: Electrical and Electronics Equipment

EV: Electric Vehicle

ICP: Inductively Coupled Plasma

LFP: Lithium Ferro-Phosphate

LIB: Lithium-ion Battery

LMO: Lithium-Manganese Oxide

LTO: Lithium-Titanium Oxide

NCA: Nickel-Cobalt-Aluminum

NMC: Nickel-Manganese-Cobalt

NMP: N-methyl-2-pyrrolidone

OEM: Original Equipment Manufacturer

PTFE: Poly Tetra Fluoro Ethylene

PVDF: Poly Vinylidene Fluoride

SEM: Scanning Electron Microscope

SX: Solvent Extraction

TM: Transition Metals (in this study, this refers to nickel, cobalt and manganese)

XRD: X-Ray Diffraction

CHAPTER 1

INTRODUCTION

The demand for energy has increased in recent years because of technological developments, increase in world population and changing lifestyles. With decreasing fossil fuel resources, the world require more renewable energy sources.[15]

Unreliable electricity generation is one of the disadvantages of using renewable energy sources. As a result, more energy have to be be stored for compensating short-term changes in electricity supply. Lithium-ion battery (LIB) is a solid alternative to be future energy storage by reason of its great energy density, specific energy, and strong rechargeability.[27]

This is not unexpected, as portable devices such as laptops, smartphones, and tablets rely heavily on LIBs for energy storage. Also, LIBs are prevalent in both personal and commercial uses[35] because they are the best attractive energy storage equipment to be used in EVs and a good choice for stationary storage solutions.[34]

Lithium-ion batteries have a lifespan and are defined by the number of cycles. The cycle occurs with one full charge and one full discharge; the battery completes one cycle after charging and then discharging. In parallel with the increasing amount of LIB usage, the amount of waste LIBs also increases.[24]

Battery cells consist of anode, cathode, separator and electrolytes. On the anode and cathode, copper foil and aluminum foil are used as current collectors, respectively. Active materials are plastered on these current collectors. Graphite, graphite/silicon or lithium titanate (LTO) is generally used as the active material at the anode. At the cathode, the active material chemistry is very diverse. Some of these are lithium cobalt oxide (LCO), nickel cobalt aluminum (NCA), nickel manganese cobalt

(NMC), and lithium ferro-phosphate (LFP). PE and/or PP microporous polymeric membranes are generally used as the separator material.[25]

In addition to graphite, lithium, and cobalt, which are included in lithium-ion batteries and defined as strategic-critical raw materials in the world, aluminum, nickel, manganese, copper, and some rare earth elements need to be recovered and re-evaluated. In addition to economic factors, some of these elements are considered critical raw materials because their reserves are meager in the world, and the high costs of mining activities and the increasing need for these elements make recycling of waste LIBs mandatory.[2]

High Li, Ni, Co, and Mn content of the applied metals is one reason for this economically motivated requirement. Used LIBs typically comprise 5-20% cobalt[72] and 5-10% nickel. 5-7% lithium Li, 5-10% other metals (copper, aluminum, iron, etc.), 15% organic compounds and 7% plastic in terms of weight.[18]

Within the scope of this study, a closed-loop approach for recovery of aluminum, lithium, nickel, cobalt and manganese, which are the raw materials in the cathodes of waste LIBs, and cathode active material synthesis via co-precipitation methods with these raw materials have been studied and characterized.

This thesis aims to show that valuable raw materials can be recovered from LIBs and they can be converted back into cathode active material. So that a closed-loop cycling of LIBs is targeted.

CHAPTER 2

LITERATURE REVIEW

2.1 Lithium-ion Batteries

LIBs, known as secondary batteries, are rechargeable electrochemical cells that can be used repeatedly. Studies carried out in the last half-century are continuing. Manufacturers are primarily concerned with maximizing efficiency and minimizing costs when developing the latest lithium-ion battery technology. Like conventional batteries, LIBs use chemical processes to store and transmit energy. The movement of Li^+ across the cathode and anode of this battery (with the aid of electrolytes) results in energy transfer. LIBs already dominate the portable electronic and electric vehicle (EVs) markets. The main reason is that they have high energy per unit mass, can work in a high voltage window, have a very low self-discharge rate, show negligible memory effects, and lose energy in an extremely gradual way when not in use.[2]

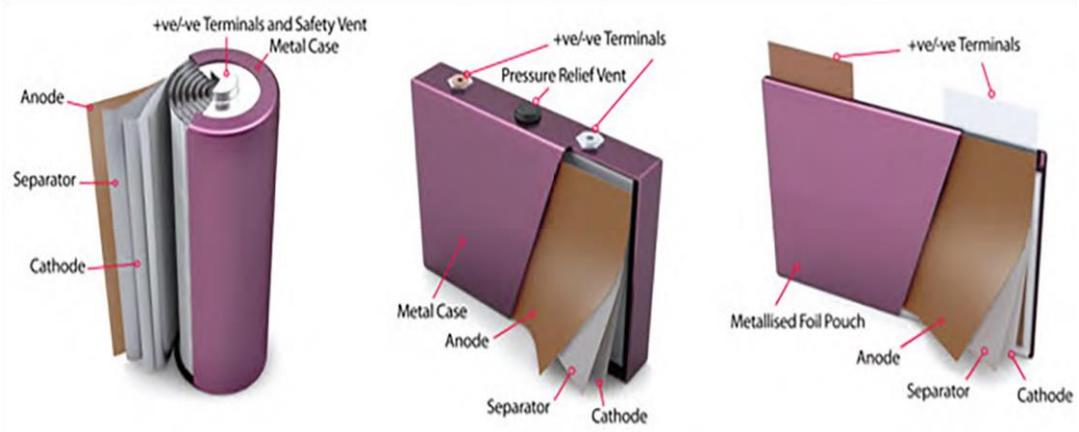

Figure 2.1. Structure and components of several lithium-ion battery cell types. The left one is cylindrical, the middle one is prismatic, and the right one is pouch-shaped.[3]

The cell is a particular component that generates power. It consists of a cathode, an anode, an electrolyte-immersed separator, and a durable case.[2] Figure 2.1 shows how LIBs can take various forms, such as cylindrical or pouch cells, depending on the needs of a particular application (i.e., at a single cell, module, or package level). However, the chemistry of the cathode active material is the most common consideration in distinguishing various types of LIBs. The first commercially successful type of LIB with liquid electrolyte is lithium cobalt oxide (LCO), which uses layered $LiCoO_2$ as the negative electrode, and uses graphite as the anode. Chemical structures are based on cathode chemistry. The most widely known types are: $LiCoO_2$ (LCO) which is coded by manufacturers as "ICR", $LiMn_2O_4$ (LMO) coded by manufacturers as "IMR", LiNixMnyCozO4 (NMC) coded by manufacturers as "INR", $LiFePO_4$ (LFP) coded by manufacturers as "IFR". Manufacturer codes are like ICR = lithium cobalt oxide cylindrical cell, I = lithium ion, C =cobalt oxide cathode, R = round cell type.[29] Figure 2.2 shows an example of these.

Figure 2.2. Cylindrical cells of Samsung company. Samsung 35E is the name, 18650 is cell type, 3500 mAh is capacity(energy), and 8A is the maximum continuous power rating. INR abbreviation stands for NMC type cathode chemistry.[3]

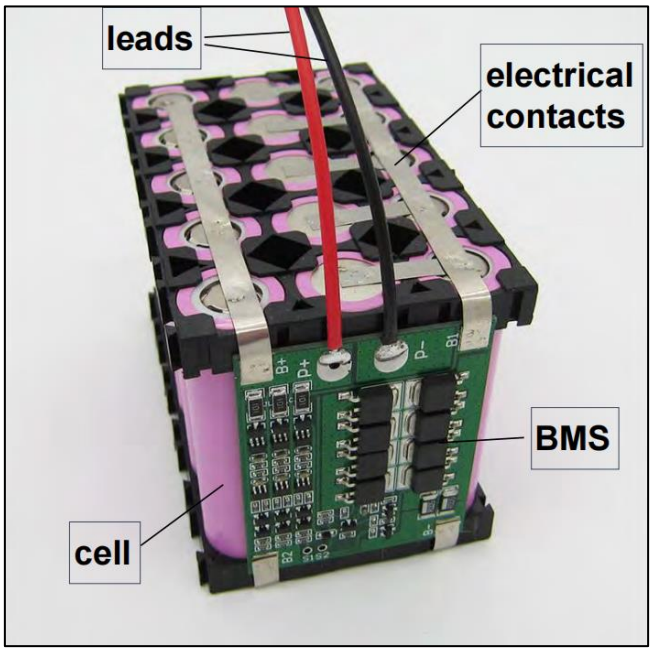

Figure 2.3. A battery pack that contains cells and electronic parts.[3]

Organic solvent electrolytes based on the $LiPF_6$ compound now dominate the market due to their superior ion conductivity. Between the anode and the electrolyte, it supports to form a solid-electrolyte-interphase (SEI), and provide a shield on the aluminum which is the current collector at the cathode.[15] Graphite anode is another common component in LIB cells.

As seen in Figure 2.3, a battery pack comprises battery modules [31], while battery module comprises of battery cells that can be connected in series and/or parallel.[4]

While the cathode material composition underwent significant changes, graphite remained the most used anode material. $LiCoO_2$ has a stable discharge capacity and is very easy to make. However, the creation of an alternative cathode was prompted by the relatively high prices and safety and environmental concerns over Co or Li mining, both of them are listed on the European Commission's Critical Raw Materials list in 2020.[4] Therefore, the trend for the coming decades is to either use

other technologies or reduce the amount of Co (for example, the stoichiometric amount of Ni:Mn:Co from NMC622 to NMC811 6:2:2 and 8:1:1, respectively).

With its excellent structural stability and long service life, lithium iron phosphate (LFP) batteries are recently the preferred option over NMC or LCO batteries. LFPs have so far been used much less frequently in sizeable electric vehicles than in small EEEs because they have low rated voltage relative to other LIBs and poor energy density.[30] Nonetheless, LFP batteries have become very important today and their share in the market is gradually increasing because they are cheaper than other LIBs in terms of raw materials. For this reason, LFP batteries are under a very fast-paced development.

On the other hand, due to the lack of cobalt, lithium manganese oxide (LMO) provides high charge/discharge rate and potential. It is also low-cost to manufacture and has little negative effect on the environment.[2] As a standalone component or in conjunction with NMC, LMO have found usage in various portable electronics, small EEEs, and electric cars such as the Chevy Volt, BMW i3, and Nissan Leaf.[2] NCA and NCM type LIBs now have the most significant energy densities. Nickel rich chemistry provides high energy density and specific capacity while lowering prices relative to cobalt. They are widely used by Auto OEMs such as BMW, BYD Auto, Renault, Tesla, Volkswagen, etc. In contrast, ni-rich cathodes have shorter cycle life and made battery thermally unstable. Furthermore, they likely cause problems like potential drop, poor rate capacitance, capacitance loss, and poor coulomb efficiency, and transition metal dissolution. The only widely used form of LIB that uses LTO instead of graphite as the anode material is the lithium titanate oxide (LTO) cell. Depending on the intended use, the cathodes of LTO cells may consist of LCO, LMO, NMC, or NCA. Compared to graphite anodes, LTO anodes offer several significant technological benefits, including lower energy density and exceptional speed capability at the expense of much longer life cycles (number of life cycles). However, higher manufacturing cost, that is 120-200% increased for LIBs having graphite anodes, are the most significant barrier to replace graphite with

LTO.[5] Figure 2.4 shows a broad comparison of the critical features of the various types of LIBs discussed.

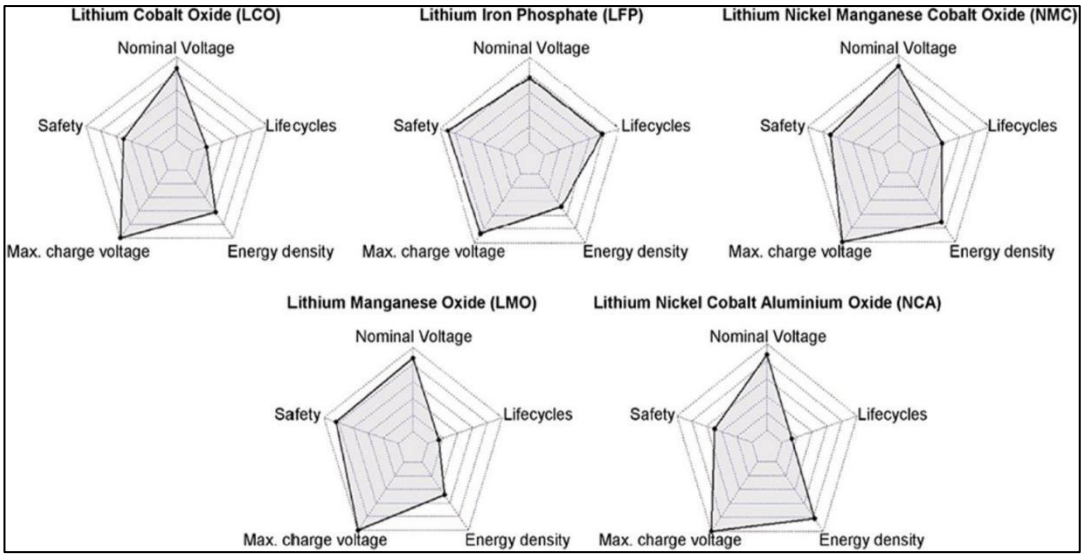

Figure 2.4. Comparison of the electrochemical properties of commonly used cathode materials and LIB types.[30]

The maximum charge/discharge voltage is indicated in a range between 0 to 4.2 V. Specified in a range between 0 °C to 300 °C, the thermal runaways' most unstable operating point determines the ultimate level of safety. Energy density, which ranges between 0 and 280 Wh/kg of a cell, measures the amount of energy a particular battery can hold. A LIB's cycle life is specified in between 0 to 4000 complete charge-discharge cycles and roughly corresponds to the estimated lifespan of a LIB type.[2]

Table 2.1 An overview of the most widely used LIBs and their application areas[9].

Battery type based on cathode chemistry	Chemical formula and stoichiometry	Nominal voltage [V / cell]	Operating range [V / cell]	Energy density [Wh/kg]	Life cycles [#]	Areas of application	Sources
Lithium Cobalt Oxide (LCO)	$LiCoO_2$	3.60	3.0-4.2	150-200	500-1,000	• Small appliances, such as smartphones, laptops, e-readers, tablets, etc.	(Chen et al., 2021; Liu et al., 2018; Ma et al., 2018; Satyavani et al., 2016; Wang et al., 2020; Yan et al., 2020)
Lithium Iron Phosphate (LFP)	$LiFePO_4$	3.20	2.0-3.65	90-160	2,000-7,000	• Small appliances, such as power tools, medical equipment, hobby gadgets, etc. • Battery electric vehicles (BEVs), such as Tesla Model 3, Nissan Leaf, Porche Taycan, and others	(Chen et al., 2021; Lander et al., 2021; Liu et al., 2018; Liu et al., 2011; Satyavani et al., 2016; Vonsien and Madlener, 2020)
Lithium Manganese Oxide (LMO)	Li_2MnO_3	3.70	3.0-4.2	100-150	400-750	• Small appliances, such as power tools, etc. • Medical equipment • BEVs (combined with NMC types)	(Chen et al., 2021; Kim et al., 2016; Liu et al., 2018; Satyavani et al., 2016; Thackeray, 1997; Weng et al., 2020)
Lithium Nickel Cobalt Aluminium Oxide (NCA)	$LiNi_{0.8}Co_{0.15}Al_{0.05}O_2$	3.70	3.0-4.2	200-260	400-1,000	• BEVs mostly produced by Telsa, such as "Model 3", or "Model X"	(Chen et al., 2021; Chen et al., 2004; Liu et al., 2018; Toggasaki et al., 2020; Vonsien and Madlener, 2020; Wang et al., 2016; Xu et al., 2015)
Lithium Nickel Manganese Cobalt Oxide (NMC)	$LiNi_xMn_yCo_zO_2$ (NiMnCo = 1:1:1, 6:2:2, or 8:1:1)	3.70	3.0-4.0	160-230	2,000-3,000	• BEVs, such as "BMW i3", "Audi e-tron GE", "BYD Yuan EV535", "BAIC EU5 R550", "Chevrolet Bolt", "Hyundai Kona Electric", "Jaguar I-Pace", "Jiangling Motors JMC E200L", "NIO ES6", "Nissan Leaf S Plus", "Renault ZOE", "Roewe Ei5", "VW e-Golf", "VW ID.3" etc. • Small appliances, such as smartphones, laptops, etc. • Battery storage power stations	(Chen et al., 2021; El Mofid et al., 2014; Liu et al., 2018; Maheshwari et al., 2018; Sun et al., 2020; Vonsien and Madlener, 2020; Zheng et al., 2016)

As a result, as shown in Table 2.1, Auto OEMs mostly use NCA, NMC, and LTO batteries. For instance, the composition of NCM altered from 1:1:1 ($LiNi_{1/3}Mn_{1/3}Co_{1/3}O_2$) to 6:2:2 ($LiNi_{0.6}Mn_{0.2}Co_{0.2}O_2$) by 2000 to 2010. More recent discoveries from 2010 to the present tend towards 8:1:1 stoichiometry ($LiNi_{0.8}Mn_{0.1}Co_{0.1}O_2$). Besides, novel anode materials like graphene or other nanocomposites may be utilized to prevent anode rupture from frequent charge and discharge cycles or to diminish the heat generated from LFP and LMO. In conclusion, it is essential to highlight that future generations of LIBs will impact the battery industry's supply chains and recycling procedures. Consequently, they should be taken into account. Collection, which can significantly impact the final product quality, is the first step in the entire process chain. In addition, a battery needs electronics, casing, and electrolyte, in addition to active elements, all of which must be considered when recycling the battery, as shown in Table 2.2.

Table 2.2 Amount of materials needed for three different compositions of NMC li-ion batteries in 1 kg battery pack.[6]

	NMC111	**NMC622**	**NMC811**
Cell materials	kg	kg	kg
Active Cathode Material	0.287	0.263	0.253
Graphite	0.160	0.171	0.168
Carbon black	0.020	0.018	0.014
Binder (PVDF)	0.025	0.024	0.029
Copper	0.134	0.134	0.131
Aluminum	0.069	0.069	0.068
Electrolyte: $LiPF_6$	0.018	0.018	0.021
Electrolyte: Ethylene Carbonate	0.050	0.050	0.057
Electrolyte: Dimethyl Carbonate	0.050	0.050	0.057
Plastic: Polypropylene	0.012	0.012	0.011
Plastic: Polyethylene	0.003	0.003	0.003
Non-cell materials			
Copper	0.003	0.002	0.003
Aluminum	0.184	0.186	0.187
Steel	0.007	0.004	0.006
PET	0.005	0.004	0.005
Electronics	0.037	0.037	0.038

For example, Arnberger et al. found that when two battery modules from end-of-life EVs are disassembled, they typically have 66% cells by weight, 17% by weight enclosure, 4% by weight electronics, and 3% by weight cables, and 10 weight percent additional ingredients.[22] The most worthy LIB part that can be recovered is the cell itself due to the fact that it comprises both cathode and anode, and contains active materials that can be as high as 60%. Whether the casing material is a heavy steel alloy, an aluminum alloy, or a lighter multi-layer composite material containing plastic will determine how much it weighs. The anode and cathode, which can make up 39% of the module weight, are generally copper and aluminum metal foils. Given the complex composition, it is already possible to envision that particular waste pretreatment technologies are necessary for separating organic materials like polymer casings and adhesives from metal parts and then process them using highly specialized metal recovery and refining technologies.

2.2 Layered Cathode Materials For LIBs

Layered cathode materials include lithium cobalt oxide (LCO), lithium nickel oxide (LNO), lithium nickel manganese cobalt oxide (NMC), and lithium nickel cobalt aluminum oxide (NCA).[5] All layered cathode structures are similar to each other, but there are variations in the lattice parameters. There are generally high charge/discharge rates because lithium ions have greater mobility than other cathode types in a 3-dimensional layered structure. LCO is the first commercially available layered cathode type because it is easy to synthesize, has good cycle life, and gives high capacity. It is still widely used today. Its experimental capacity in the literature is 247 mAh g^{-1}.[28]

Emergence of other layered cathode types was due to the fact that mining of cobalt is very harmful to the environment and requires high costs to achieve.

LNO has similar advantages to LCO, but the disadvantage is that an irreversible phase transition occurs during charge-discharge. The radii of nickel (Ni^{+2}) and lithium (Li^{+1}) ions (0.69 Å) and (0.76 Å), respectively, are close to each other.

Therefore, during charge-discharge, nickel ions occupy the sites where lithium ions are expected to enter, causing a loss of capacity. This phenomenon is called cation mixing or cation disorder. For this reason, LNO is far from being a very suitable candidate for industrial use. To avoid these disadvantages of LCO and LNO batteries, NCO type cathode chemistry has been studied. Studies have shown that this cathode type has better capacity and reversibility than previous cathode types in various compositions. However, NCO cathodes with low cost and high capacity retention could not be synthesized for industrial use. For this reason, researches continued to add aluminum or manganese elements to the NCO cathode chemistry. NCA type cathodes were synthesized by adding aluminum. In this way, more stabilization has been gained to the structure. This stabilization has also increased the thermal stability. TESLA was the first company to use NCA-type cathodes in their electric vehicles. Apart from this, NMC type cathodes were investigated with manganese element. Electrochemical stability was observed to increase with the addition of manganese element to NCO type cathodes, but it was observed that it also decreased the electrical conductivity. Figure 2.5 depicts the ordered and disordered phases of layered lithium metal oxides along with the structural changes they go through.

In XRD analysis, the ratio of I_{003}/I_{104} is expected to be more than 1.7 on a standard NMC cathode because cation mixing occurs on the 104 plane.[30] For this reason, these (104) plane peaks should be much less than (003) peaks at the cathode, which has a high performance expectation.

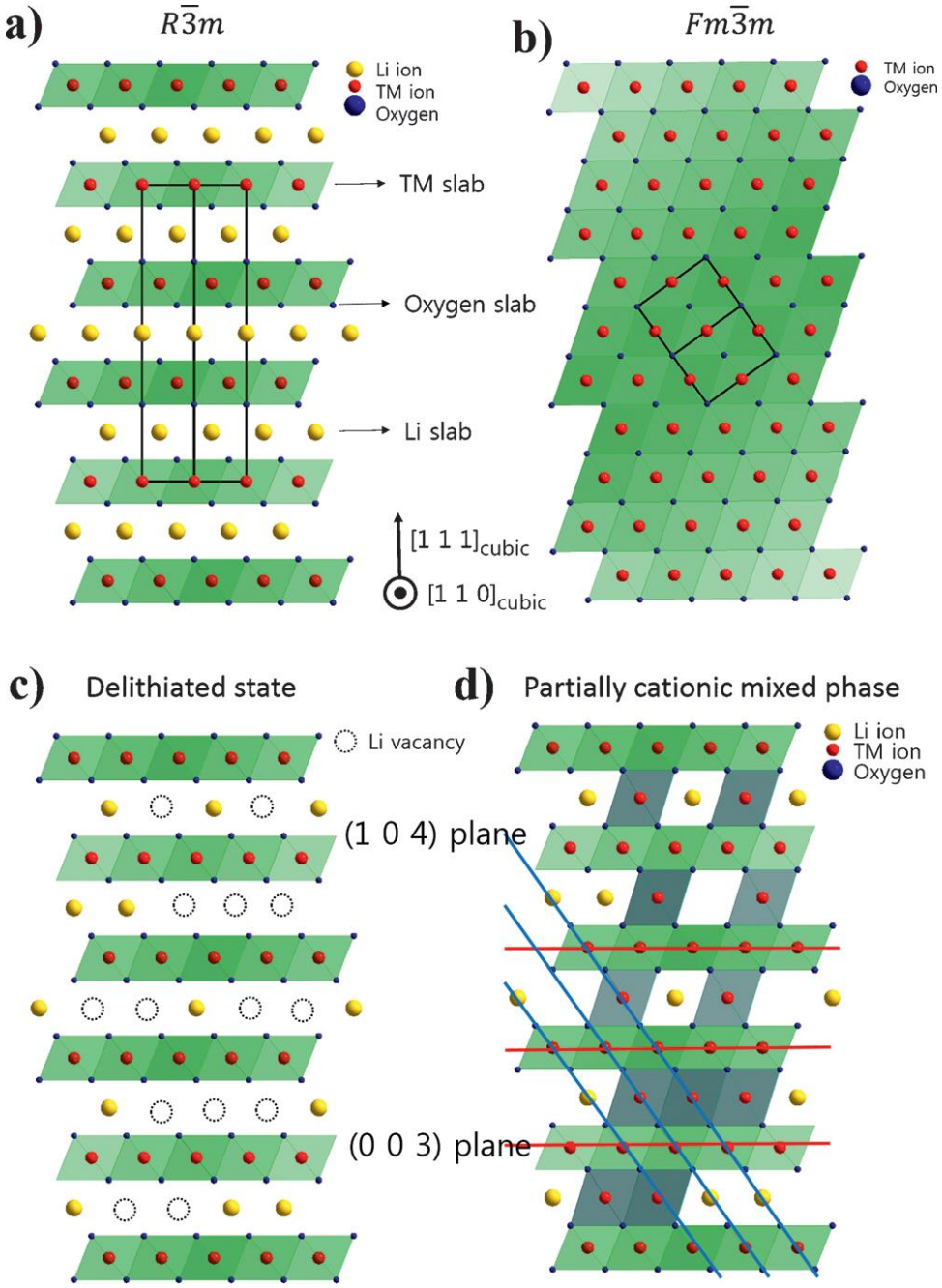

Figure 2.5. a) The ordered structure. b) Cation disorder, c) Lithium vacancies in highly charged state, d) Partially cation mixed phase containing TM ions in Li slab. Yellows are depicted as lithium atoms, transition metals in red, and coordinated oxygen atoms in dark blue.[11]

2.3 Statistics of LIB Market

As the electric vehicle (EV) market grows and more LIBs are made, infrastructure and plans are needed to deal with spent LIBs and to recycle valuable materials in the cathode. Based on a material flow analysis study, EV battery packs can produce from 0.33 to 4 million metric tons of LIB in between 2015 and 2040, depending on how conservative or extreme their estimates are.[6] The forecast takes into account different estimates of how many EVs will be sold, how long the LIB cathodes will last (statisticially 8-10 year)[6], and how many cells are in a module. Assuming all metals, Al, Cu, Ni, Co and Fe are collected and reused, estimated amount of 1.3 billion kg spent LIB from EVs gives a commodity of around $3 billion.[25] LIB recycling is also essential for keeping valuable resources in good condition.

The sales of electric vehicles are increasing around the world and the demand for them is increasing day by day as can be seen from Figure 2.6.A. In line with this demand, manufacturing of EVs is also increased as shown in Figure 2.6.C. The raw materials required to produce the batteries of these vehicles are at a supply level that cannot meet the worldwide demand.[27] For this reason, the raw materials used in battery production are getting more and more valuable day by day as it can be seen from Figure 2.6.B. The chemical diversity of the cathode active materials and ratios of metals in the same type of cathode to each other also vary according to the area of use or cost as shown in the Figure 2.6.D.

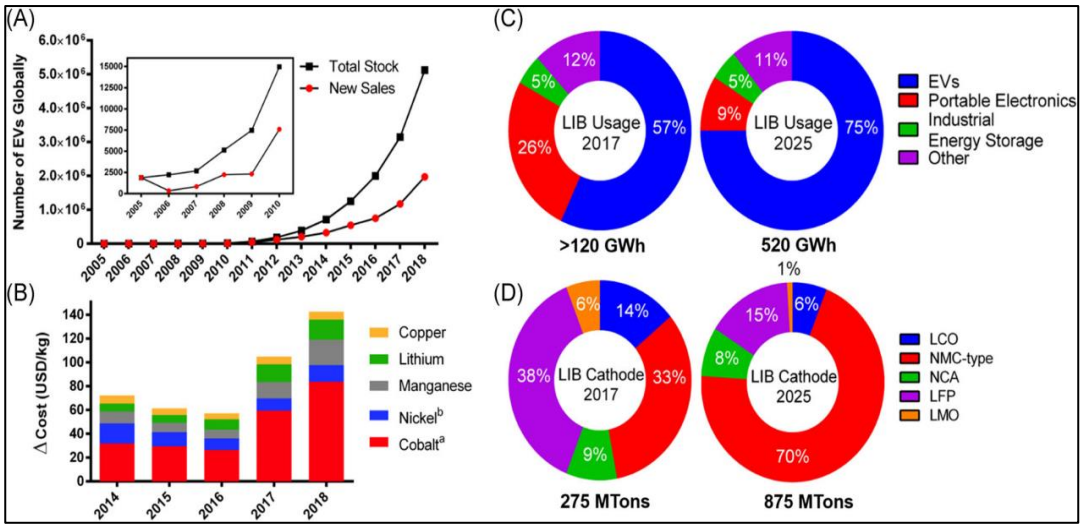

Figure 2.6. A) Worldwide new EV sales to date. B) Price of valuable metals used in LIBs in 2018 (shown in the size of a bar) from the US Geological Survey. LIB market share projections based on (C) usage and (D) cathode stoichiometry. The estimate is based on the idea that Tesla, Inc. will be the only major EV maker to use NCA cells in 2025.[6]

CHAPTER 3

EXPERIMENTAL PROCEDURE

For closed-loop recycling of waste batteries, there is primarily a discharge stage. After this stage, there is the dismantling stage, so the batteries are separated into their components. From here on, two main approaches, namely alternative process routes, have been studied. One of them is the method of disengagement and direct utilization of cathode active materials, and the other is method of acid leaching for direct co-precipitation with the leachate solution. These alternative approaches and methods can be followed on the flow chart in Figure 3.1.

Three alternative methods have been studied for the method of disengagement and direct utilization of cathode active materials. These are pyrolysis method, dissolution of PVDF method and dissolution of aluminum foil method.

The method of acid leaching for direct co-precipitation with the leachate solution starts by leaching optimization of the dismantled cathode active material with various acid solutions. Acid types, reductant presence and their types, concentration of both acid and reductant, leaching time and leaching temperature parameters were studied. After the leaching process, filtration was performed and leachate, that is, pregnant leach solution, was obtained. Pregnant leach solution contains aluminum. For this reason, in the purification stage, NaOH solution was prepared and dosed into PLS, and aluminum in the solution was precipitated in the form of aluminum hydroxide and removed from the solution, and aluminum hydroxide was obtained in solid phase by filtration. After the aluminum was removed, a solution containing only lithium, nickel, cobalt and manganese was obtained. The adjustment stage is the addition of metals to the solution according to the NMC stoichiometry desired to be synthesized after the stoichiometric ratio of

this solution is determined by ICP-OES analysis. In the co-precipitation stage, cathode active material precursor synthesis is made and filtration process is applied. Lithium remains in the filtrate and this lithium is recovered in the form of lithium phosphate with the help of sodium phosphate salt.

With the help of the flow chart in Figure 3.1, the experimental route is as briefly mentioned above. Details of the studies are explained in the following headings.

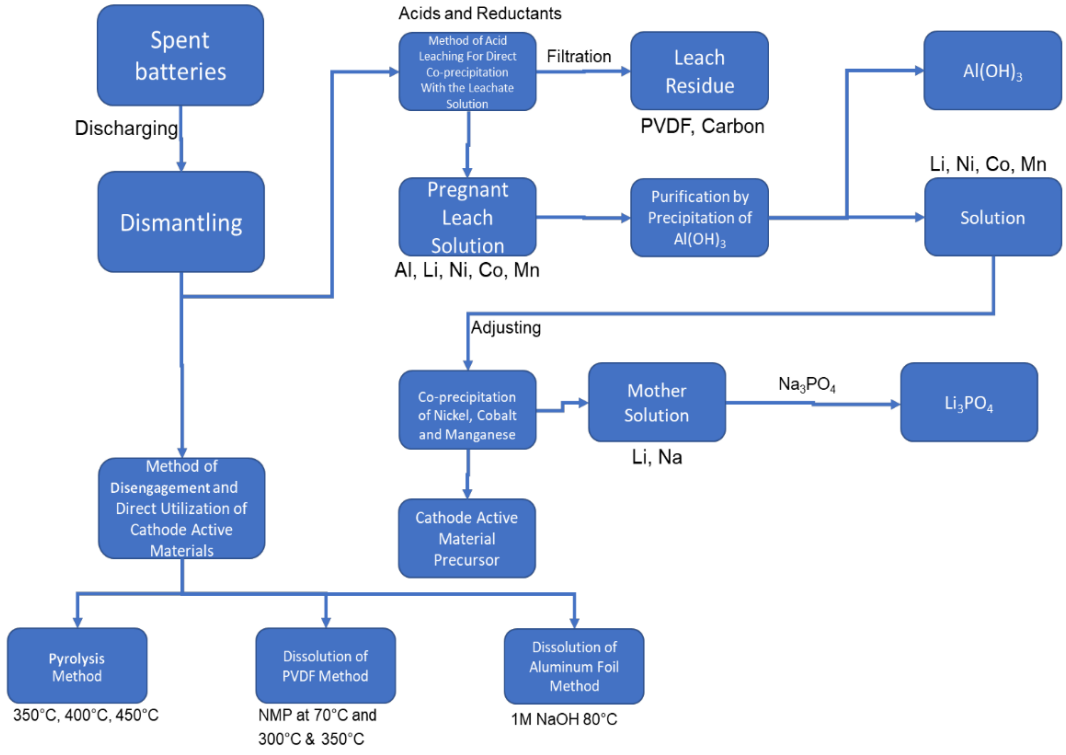

Figure 3.1. Flow chart of the approaches and experimental proccesses.

3.1 Materials and Reagents

HNO_3, H_2SO_4, H_3PO_4, and HCl were used as acid reagents supplied by Sigma Aldrich. H_2O_2 and SO_2 were used as reducing agents and were provided by Merck and Linde, respectively. NaOH was supplied in pellet form, and NH_4OH was provided as a solution by Merck. NMP solvent was supplied from Sigma Aldrich.

Li_2CO_3, $NiSO_4 \cdot 6H_2O$, $CoSO_4 \cdot 7H_2O$, and $MnSO_4 \cdot H_2O$ were supplied from Merck. All the chemicals were reagent grade and used as received without any further purification.

Waste lithium-ion batteries were collected from local phone and laptop repairs. These were spent battery packs or cells discarded because they were thought to be expired. In this thesis, spent LIBs containing layered cathode active materials which are NMC, LCO and NCA were utilized for experiments conducted because they have various materials in the cathode active material, such as nickel, manganese, cobalt, aluminum and carbon. Hence, recycling this cathode chemistry has more complexity relative to others. They were a mix of cylindrical 18650 and pouch cells.

3.2 Structural Characterization

The crystal structure of materials was analyzed by an X-Ray Diffractometer (XRD, Bruker D8 Advance) using Bragg-Brentano geometry with Cu-Kα radiation. The XRD patterns were collected with a 2°/min scan rate.

Morphology of materials was investigated by scanning electron microscopy (SEM, Nova NanoSEM 430) using 20kV accelerating voltage.

Particle size measurements of the materials were performed using a laser diffraction particle analyzer (Mastersizer 2000), where the powders were dispersed in ethanol.

FTIR analyses were performed using an infrared spectrometer (Bruker IFS 66/S).

3.3 Chemical Characterization

Energy Dispersive Spectroscopy (EDS) was performed as the first step for the chemical analyses. EDS is an easy and convenient method to qualify and quantify the chemical ingredients of the produced materials. However, it can detect elements

with a higher atomic number than 10. Therefore, inductively coupled plasma-optical emission spectrophotometer (ICP-OES Agilent 5900 SVDV) and inductively coupled plasma–mass spectrometer (ICP-MS Perkin Elmer Nexion 350x) was used to have more accurate results.

pH meter used for determining the pH of liquids was Mettler Toledo pH meter (Seven2Go Cond meter S7).

3.4 Electrochemical Characterization

Charge-discharge behavior, discharge capacity, and cycle life were measured using a potentiostat/galvanostat (Bio-Logic Instruments VMP-300). The electrochemical cells were cycled at 0.5C rates (1C=170 $mAhg^{-1}$) within 2.7-4.2 V potential windows for NMC-622 cathode material and 0.5C rates (1C=155 $mAhg^{-1}$) within 2.7-4.3 V potential windows for NMC-111 cathode material.

3.5 Discharging

Spent lithium-ion batteries procured from local markets were soaked seperately in 1%, 2%, 3%, 4%, and 5% by weight NaCl solutions and waited 24 hours. After this period, a representative amount of different batteries from each batch were tested with a multimeter to determine whether they totally discharged or not.

3.6 Dismantling

All the plastic parts and casings were dismantled manually one by one, and opened cells were uncurled. Cathode plates were cut with a scissor in 1x1 cm.

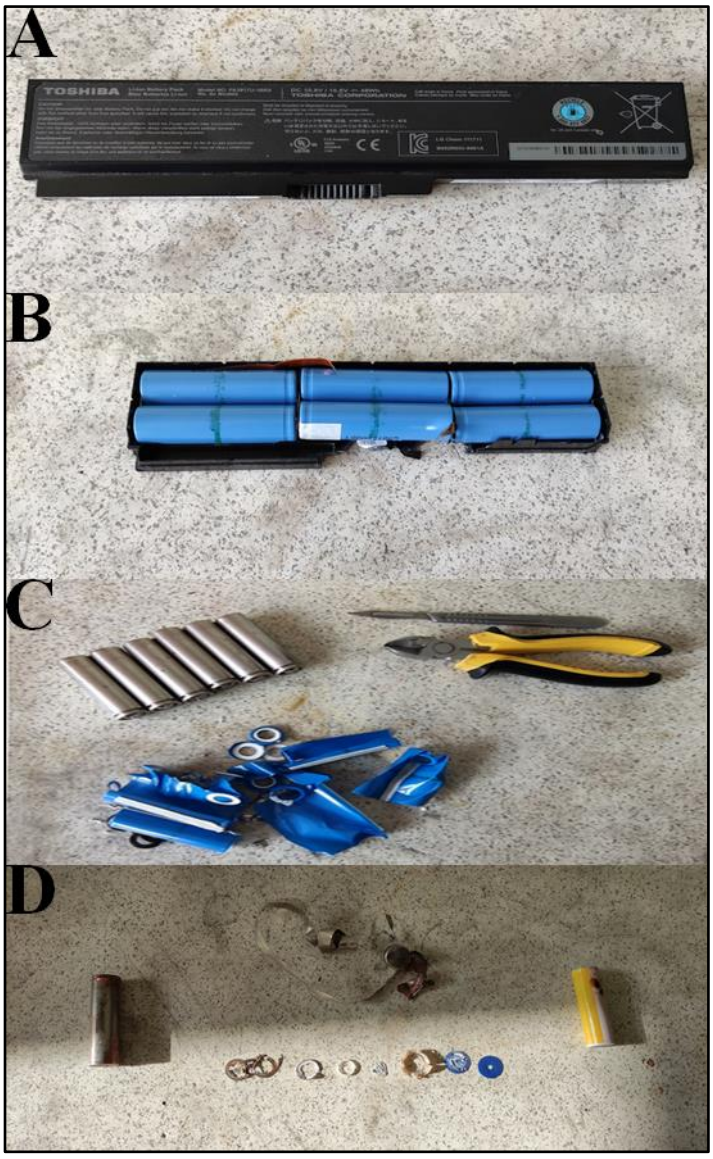

Figure 3.2. Dismantling of 18650 NMC cells. A) Battery pack comprising EoL LIB cells which was used as TOSHIBA laptop battery. B) Broken plastic

pack casings. C) Electronic connections and plastic casings torn. D) Cases and electrodes separated and uncurled cells.

3.7 Method of Disengagement and Direct Utilization of Cathode Active Materials

The aim of this approach is to strip the cathode active materials of waste lithium-ion batteries from the current collector foil and directly turn them back into a sludge to prepare new electrodes. In other words, within this approach, it was aimed to produce a new electrode directly from the cathode active materials that were isolated from spent li-ion batteries. The most important promise of this approach is the direct recycling of waste lithium-ion batteries, avoiding complicated processes and high costs. In this thesis study, samples taken from NMC-111 waste lithium-ion batteries were used after they were discharged. The cathode chemistry of the waste battery was determined as NMC-111 based on ICP-OES analysis. Three different methods have been studied in this approach. They are pyrolysis method, dissolution of PVDF method and dissolution of aluminum foil method. Each of these is on the separation of active materials from aluminum foil, which is a current collector. FTIR analysis was performed to NMC-111 cathode in order to understand whether the organic used as binder was PVDF or PTFE. It was determined that PVDF was used as described in Figure 4.1 in the results and discussion chapter.

3.7.1 Pyrolysis Method

In the pyrolysis method, the aim is to pyrolyse the PVDF, which is a binder, so that the current collector foil and the active material will get rid of each other.

100 g $Li(Ni_{1/3}Co_{1/3}Mn_{1/3})O_2$ of cathode cathode actives were cut into 1x1 cm^2 size sheets and heated to 350°C, 400°C, and 450°C for 2 h in a muffle furnace, seperately.

Then, the active materials peel off Al foil by the fast stirring mixer. Finally, the recovered active materials were sifted out by a 450 mesh screen. XRD analysis then performed to the active materials.

3.7.2 Dissolution of PVDF Method

In this method, the aim is to dissolve the PVDF, which is the binder, with NMP and to filter the active materials and Al foils. The active materials should be collected by the falling of the active materials on the Al foils.

100 g of $Li(Ni_{1/3}Co_{1/3}Mn_{1/3})O_2$ electrode plate was cut into 1x1 cm^2 size sheets and added into a stirring beaker containing 200 ml NMP at 70°C. Temperature of the media was maintained at 70°C. After stirring for 3 hours, aluminum foils were removed from the solution. The solution was then filtered to collect the active materials on the filter paper. Afterwards, the particles were washed with ethanol to completely eliminate the NMP on them. Previously taken aluminum foils were also washed with ethanol to collect remaining active material on them. All the active materials were dried in air at 100°C for 1 hour. Then, dried active materials were divided into two parts and pyrolysed at 300°C and 350°C for 3 hours, seperately. Then they were grinded, and screened using a 450 mesh screen separetaly.

3.7.3 Dissolution of Aluminum Foil Method

In this method, the aim is to dissolve the aluminum foil, which is the current collector, with NaOH solution and to filter the active materials and PVDF. The active materials should be collected by sieving the filtered particles, the active materials will remain under the sieve and the PVDF will remain on the sieve.

100 g of $Li(Ni_{1/3}Co_{1/3}Mn_{1/3})O_2$ electrode plate was cut into 1x1 cm^2 size sheets and added into a stirring beaker containing 570 ml of 1 M NaOH at 80°C. Temperature

of the media was kept constant at 80°C. After mixing for 3 hours, the aluminum foils were dissolved in the solution. The solution was then filtered to collect the active materials and PVDF on the filter paper. Afterwards, they were washed using hot water to completely remove the residual alkali solution on the active materials. All the mixture of cathode active materials and PVDF were dried in air at 100°C for 1 hour. Then, dried active materials were grinded and screened using 450 mesh screen and active materials were remained under the sieve and the PVDF particles were remained on the sieve.

3.8 Method of Acid Leaching For Direct Co-precipitation With the Leachate Solution

20 g of cathode active materials were leached to produce the leach solutions in each 500 ml of four different inorganic acids, separately. These acids are HCl, H_2SO_4, HNO_3, and H_3PO_4. Reducing agents investigated were H_2O_2 solution and SO_2 gas. H_2O_2 solution was produced by dilution of the necessary proportions of 30% w/w H_2O_2 in de-ionized water. SO_2 gas was utilized by scrubbing into agitating media. By dilution of the necessary amounts of 37% w/w HCl in deionized water, HCl solutions were created. H_2SO_4 solutions were 96% w/w H_2SO_4 in deionized water, and HNO_3 solutions were 70% w/w HNO_3 in deionized water, H_3PO_4 solutions were 85% w/w H_3PO_4 in deionized water. Diluted acids were added to the reactor under agitation and temperature was set before introducing the cathode active material powders. For all the leaching experiments conducted, the solid-to-liquid ratio (S/L) and agitating speed were kept constant as a fixed parameter at 1:10 g/ml and 230 RPM, respectively. Leaching experiments were conducted initially keeping mixing time as a fixed parameter of 3 hours, but after optimizing the other parameters except S/L ratio and the agitating speed, the mixing time was also optimized. A mechanical steel agitator coated with PTFE was used for mixing.

Various factors which may affect the leaching efficiency (acid concentration, reducing agent concentration, temperature (T), and mixing time (t) were examined.

Firstly, the most suitable acid candidate among the others was determined for utilizing in leaching. To make this comparison, 500 ml of 2 molar acid solution of each acid was prepared. 20 grams of cathode active material powders were added to the mixing solutions when each reached a temperature of 80°C. After 3 hours, each was filtered and samples were taken for chemical analysis. Hydrochloric acid was superior to other acids in terms of leaching efficiency. However, by testing each acid at different concentrations and with different reducing agents, it was investigated whether there was a synergistic effect. Also H_2O_2 as a reducing agent was investigated in terms of concentration. After that, time and temperature parameters were investigated. After every leaching experiment, the leach solution and unsolved residue were separated by vacuum filtration. The concentrations of nickel, cobalt, manganese, and lithium in the leach solutions were determined by inductively coupled plasma-optical emission spectrophotometer and inductively coupled plasma–mass spectrometer. Efficiencies of leach experiments, for chemical element "i", were determined with the following equation:

$$\%E_i = \frac{C_f(i) - C_0(i)}{C_f(i)} \times 100\%$$

where $C_f(i)$ is the final concentration of metal "i" in the leach solution and $C_0(i)$ is the initial concentration of metal "i" in the initial cathode active material powder to be leached.[53]

3.8.1 Adjusting the Leachate Solution For Co-precipitation Synthesis

Pregnant leach solution (PLS) comprising Li, Ni, Co, and Mn is chemically characterized using ICP-OES, and stoichiometrical fractions of metals were determined. Then additional nickel sulfate, cobalt sulfate and manganese sulfate

which were supplied by Merck utilized as received without any further purification, added if needed to balance the PLS to reach the desired stoichiometry. Then the solution which contains the desired stoichiometry of metals was obtained. In this thesis syudy, this NMC stoichiometry was chosen to be 6:2:2. After adjustment of the TM containing solution, synthesis of the cathode active material via the co-precipitation method took place.

3.9 Synthesis of Cathode Active Material via Co-precipitation Method

In this thesis study, all cathode active materials were synthesized using the co-precipitation method. As can be seen from the schematic representation of co-precipitation in Figure 3.3., The sulfate solution comprising Li, Ni, Co, and Mn in the stoichiometry of NMC-622 and 1.5 Molar concentration was fed dropwise with a peristaltic pump simultaneously with 0.6 M NH_4OH solution and 3 M NaOH solution to adjust the pH into a 500 ml glass reactor which has 100 ml %5 v/v NH_4OH initially as a base media. Nitrogen gas is used to form an inert atmosphere by dipping into the agitating solution media to prevent the premature oxidization of metals, especially manganese. The solution containing TM and the NH_4OH solution are transferred to the reactor at 0.55 ml/min at the flow rates to be finished at the same time. The NaOH solution is added to the reactor in a controlled manner in order to keep the pH balanced at 11.2. Each solution is fed to the system with the help of peristaltic pumps. When the solution containing TM and NH_4OH solution were totally consumed, agitation and nitrogen gas flow still continued for 10 hours more to ensure the reaction was completely finished. Afterward, filtrate particles were washed with hot water in 1:10 S/L ratio five times to remove all alkali solution on them, and dried at 80°C for 24 h.

Lithiation is done using Li_2CO_3 by 5% w/w excess amount, then pre-calcination was done in a furnace at 450°C for 4 h. After pre-calcination, the calcination stage took place in a furnace at 850°C for 10 h.

After obtaining the co-precipitation products, the solution which contains lithium and sodium was saved for lithium recovery. Adding Na_3PO_4 into the solution, Li_3PO_4 precipitates was formed and by vacuum filtration they all recovered. Water solubility of Li_3PO_4 in water is 0.3 g/L at 25° so that recovering lithium in the phosphate form is very efficient than the other forms like carbonate or hydroxide.

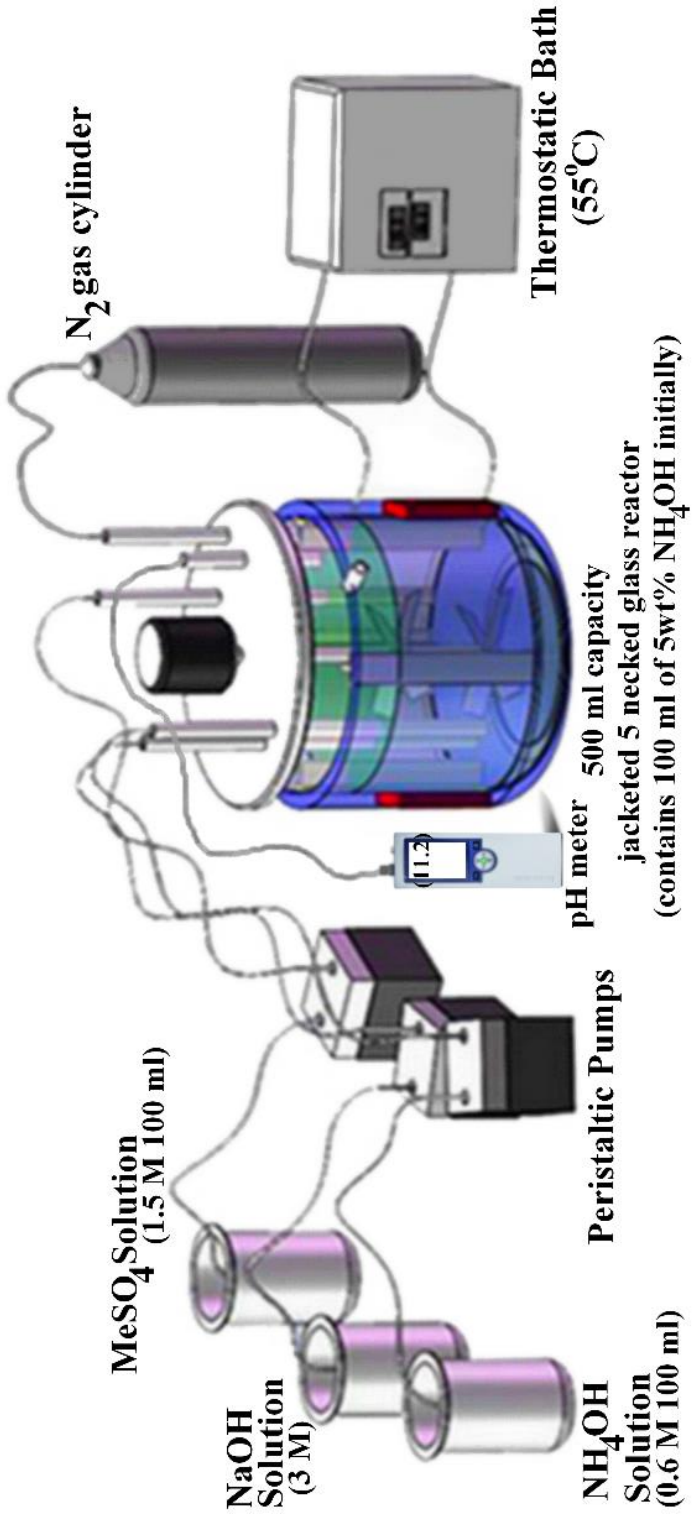

Figure 3.3. Schematic of the co-precipitation reaction.

CHAPTER 4

RESULTS AND DISCUSSION

4.1 Discharging

Spent lithium-ion batteries, which are cylindrical 18650 type and pouch type procured from local markets, were soaked separately in 1%, 2%, 3%, 4%, and 5% w/w NaCl solution to determine the concentration needed for the total discharge of batteries, and were hold 24 hours. After this period, the representative number of different batteries from each batch was tested with a multimeter and determined that discharging was done entirely with the 5% w/w brine solution. It was observed that dismantling the batteries are safer after discharge them using 5% w/w brine solution batch for 24 hour. There was no spark or flaming issues when dismantling after discharging the batteries in 5% w/w brine solution. It has been observed that the batteries taken from the solution below 5 molar brine solution can burn during the dismantling phase, even if there is a little energy left detected in the measurements with the multimeter. The knob of the multimeter was rotated to 15-20V DC voltage value. Choosing this range is sufficient as it is more than the average voltage range of the batteries, 3-4 V. The plug of the red probe is connected to the VΩmA port and the black one is connected to the COM port. The red probe was connected to the positive terminal of the battery, and the black probe was connected to the negative terminal. Fully discharged batteries were determined by looking at the values read on the multimeter.

It should also be noted that brine discharge is much safer than typical air-atmosphere discharge because batteries do not tend to flame in aqueous media, but they can heat the solution.

4.2 Disengagement and Direct Utilization of Cathode Active Material

As shown in Figure 4.1, 1410.28 cm^{-1} is the deformation vibration spectrum of the CH_2-CF_2 bond in PVDF[7]. 1194.33 cm^{-1} is the telescopic vibration spectrum of CF_2 in PVDF.[7] 864.61 cm^{-1} represents the adsorption vibration spectrum of the crystalline phase.[7] For this reason, it is clearly seen that PVDF was used as a binder in the NMC-111 cathodes that were investigated.

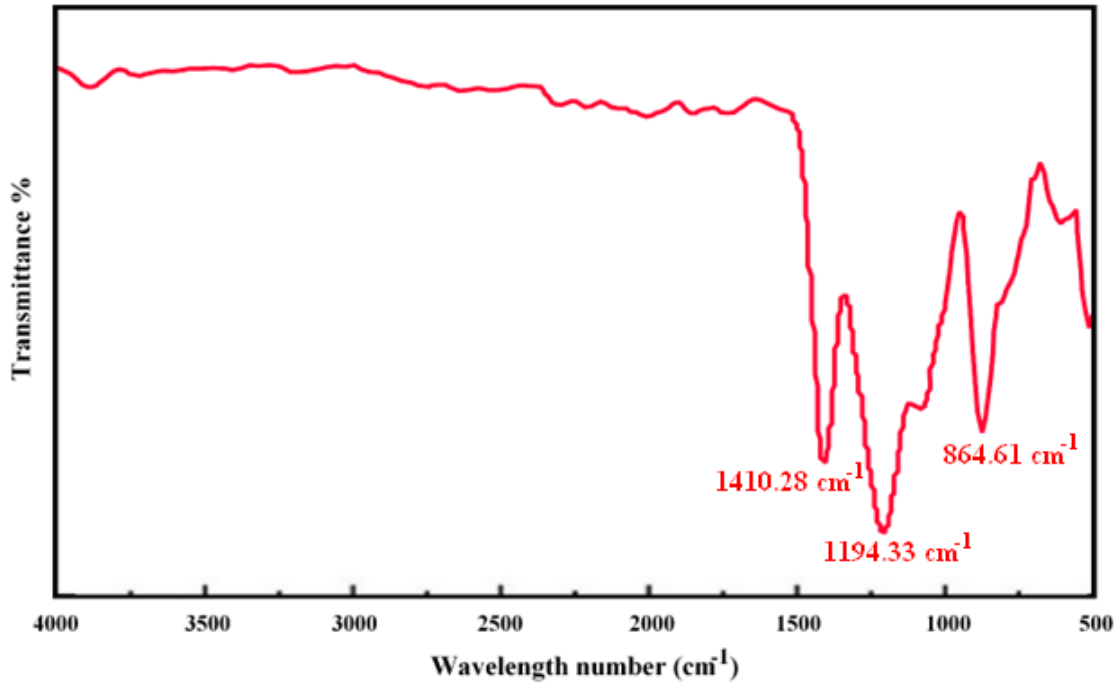

Figure 4.1. Fourier Transform Infrared Spectroscopy of NMC-111 spent LIB cathode.

4.2.1 Pyrolysis Method

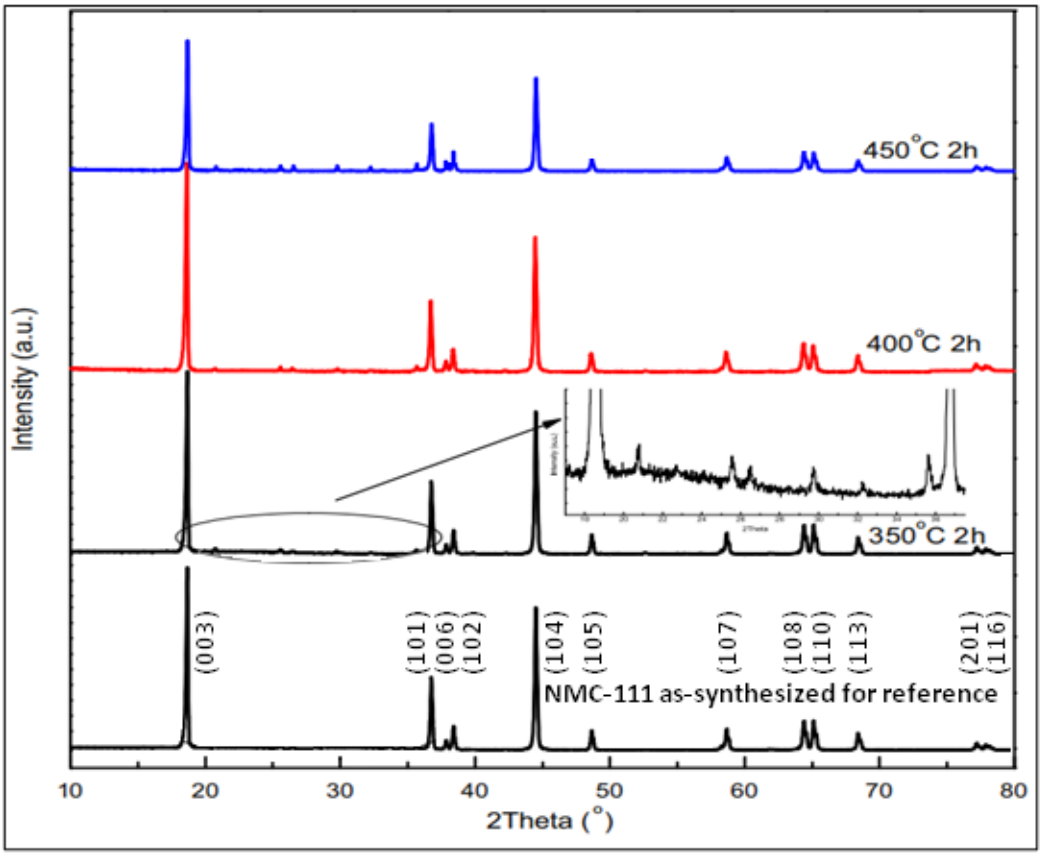

Figure 4.2. XRD patterns of the cathode active materials pyrolysed at different temperatures and the XRD pattern of the reference cathode active material that is synthesized for comparison (ICSD No:1817019 for $Li(Ni_{1/3}Co_{1/3}Mn_{1/3})O_2$).

Figure 4.2 shows XRD patterns of the cathode active materials pyrolysed at three distinctive temperatures and a reference sample at the bottom that is synthesized for comparison. There are several small peaks between 20° and 35° in the XRD pattern of each specimen as can be seen from Figure 4.2., means that $Li(Ni_{1/3}Co_{1/3}Mn_{1/3})O_2$ cathode active materials were affected after the pyrolysis process. In order to find out which component in the waste cathodes is the underlying cause of this structural change, a couple parallel test were performed. Synthetically produced and lithiated

cathode active material was placed in both crucibles in the same amount. Then only carbon black was added to one, and only PVDF to the other. Both crucibles were kept at 450°C degree for 3 hours. The peaks in Figure 4.2 signifying impurity were not observed in the XRD analysis of the carbon black added sample. This means that existence of those peaks are not due to the presence of carbon black which does not lead to neither carbothermal reaction nor self decomposition at this level of temperature.

It was seen that PVDF containing specimen shows those impurity peaks on its XRD pattern, which means that the cause of impurities is having PVDF with the $Li(Ni_{1/3}Co_{1/3}Mn_{1/3})O_2$ powders. It is concluded that the decomposition of PVDF during the pyrolysis has an effect and the reagents formed as a result of this reaction cause a change in the layered structure.

It is concluded that the decomposition of PVDF can release HF during the pyrolysis and HF obviously has an effect on the layered cathode chemistry. In order to prove that, following pyrolysis, cathode active materials were rinsed with hot water, and the existence of F^- ions is tested using calcium chloride.

As can be seen from the XRD pattern of the centrifuged white residue at the bottom of the flask in the Figure 4.3., the white residue is calcium fluroide, proves that the presence of lithium flouride in the cathode active material after pyrolysis. But from Figure 4.2, only a little change in the structure of $Li(Ni_{1/3}Co_{1/3}Mn_{1/3})O_2$ occured due to HF formation, layered structure is not entirely lost though, distinctive peaks of the layered structure are still there.

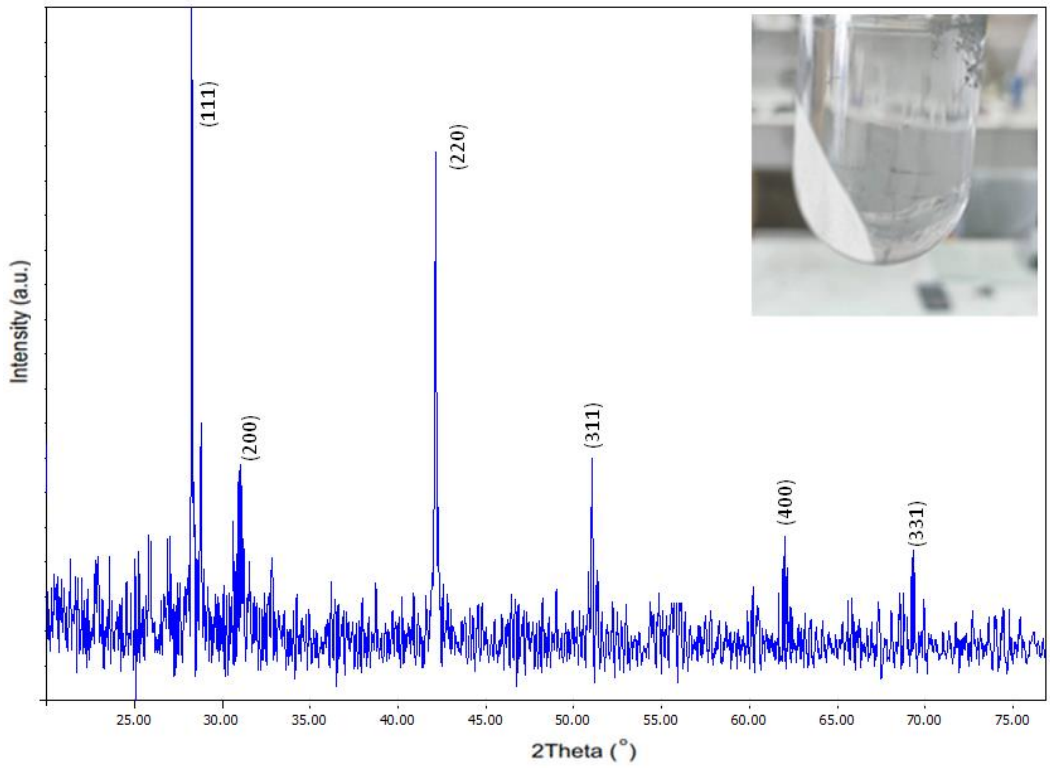

Figure 4.3. XRD pattern of the precipitated white residue which is CaF_2 particles after addition of $CaCl_2$ (ICSD No: 28730).

After the pyrolysis at 350°C, it was observed that a very small amount of cathode active material seperated from the aluminum foil indicating that PVDF has not been obliterated in this condition. After the pyrolysis at 400°C, it was observed that most cathode active material seperated from Al foil, indicating that PVDF can be removed mostly in this condition. After the pyrolysis at 450°C, it was observed that all cathode active material could fall off from Al foil indicating that PVDF can be removed completely in this condition. The above results indicate that cathode active materials can fall off from Al foil when the pyrolysis temperature is above 400°C.

The charge/discharge capacity behaviour of the cathode active materials pyrolysed at distinct temperatures can be seen in Figure 4.4. The test was carried out 0.5C charge/discharge rate considering that experimental capacity of NMC-111 cathode is 155 mAh/g (2.7 – 4.3V at 0.5C).

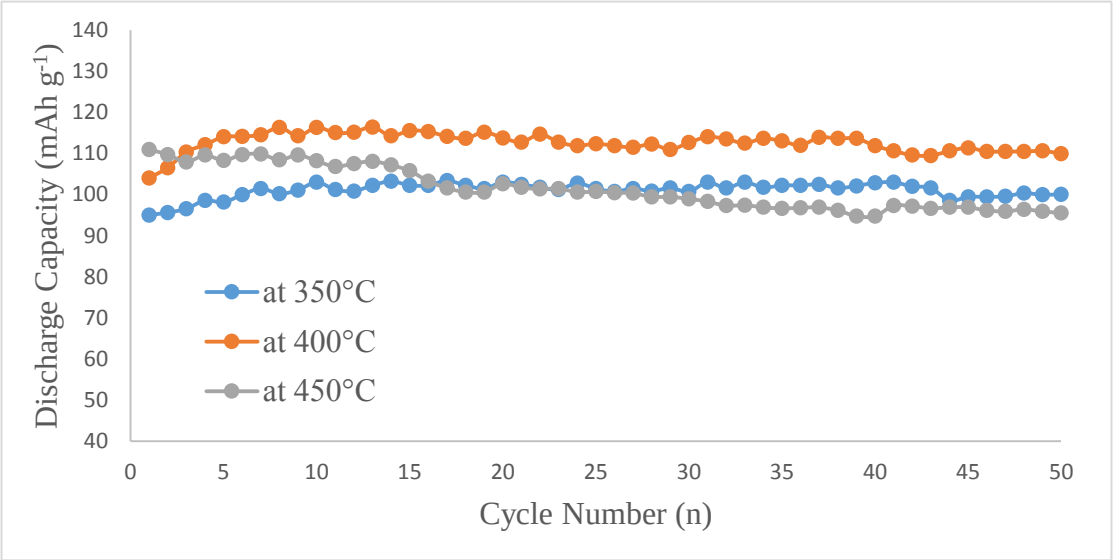

Figure 4.4. Cycle life of the cathode active materials pyrolysed at different temperatures.

The maximum discharge capacity of the cathode active materials pyrolysed at 350°C is 105 mAh g^{-1}, at 400°C is 115 mAh g^{-1}, at 450°C is 110 mAh g^{-1}.

It has been seen in the cycle life tests of the electrodes produced with cathode active materials obtained by pyrolysis that their discharge capacities are significantly lower than the as-synthesized $Li(Ni_{1/3}Co_{1/3}Mn_{1/3})O_2$ cathode active material (155 mAh g^{-1}) [1].

It is seen in Figure 4.4 that the discharge capacity increases when the pyrolysis temperature is increased from 350°C to 400°C. However, it was observed that the pyrolysis at 450°C had a significant negative effect on the cycle life and discharge capacity, which is related to the decomposition of $Li(Ni_{1/3}Co_{1/3}Mn_{1/3})O_2$.

As a result of the above results, it has been clearly seen that the pyrolysed NMC has a negative effect on the discharge capacity and cycle life. Therefore, the pyrolysis method is found to be unsuitable for recovering $Li(Ni_{1/3}Co_{1/3}Mn_{1/3})O_2$ cathode active materials for direct utilization due to the fact that decomposition of PVDF leads to HF formation which is hazardous to the environment and human health also reacts with the active material and leads to decrease in electrochemical performance.

4.2.2 Dissolution of PVDF Method

Except for the pyrolysis method, the dissolution of PVDF method is another way to eliminate PVDF from cathode active materials. Typical solvents such as N-methyl-2-pyrrolidone (NMP), Dimethylacetamide (DMAC), and N,N-Dimethylformamide (DMF) capable of dissolving it, but NMP was preferred among the others because of the lower price, superior solubility, and re-usability of NMP. Figure 4.5 is IR spectrums of the cathode active material that underwent dissolution of PVDF method with NMP solvent (non-pyrolysed one). It can be seen that several small spectra which are the typical absorption spectra of PVDF (such as 1630 cm^{-1}, 1402 cm^{-1}, 1191 cm^{-1} and 881 cm^{-1}) in non-pyrolysed cathode active materials, implying that PVDF is not entirely eliminated using only dissolution of PVDF method. Furthermore, the spectrum at 3455 cm^{-1} is from the residual water bond to structure. It was investigated whether residual PVDF causes performance loss of cathode active material because the presence of PVDF can affect the electro-chemical functions of the cathode active material.

In consideration of these, subsequently, parallel pyrolysiss at 300°C and 350°C degrees were applied to further removal of residual PVDF as well. The aim of using lower pyrolysis temperatures than those mentioned in the previous parts were chosen to evade or minimize the risk of HF formation which can be formed from the decomposition of PVDF.

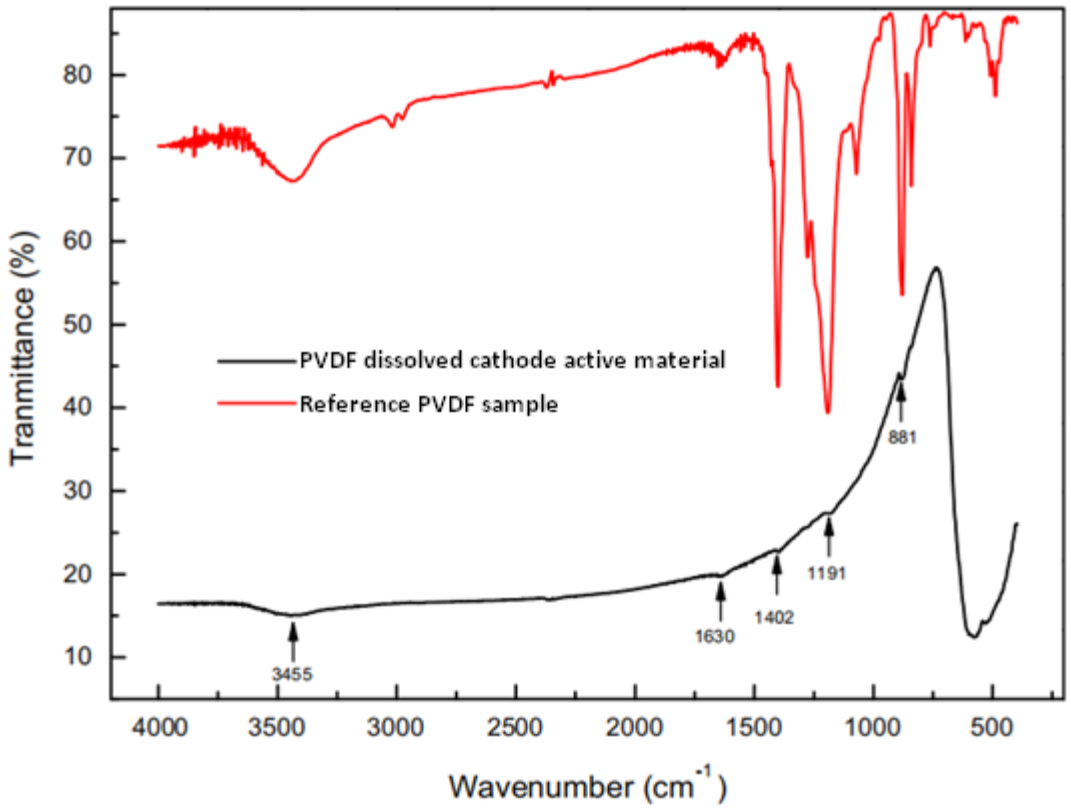

Figure 4.5. IR spectrums of the cathode active material that underwent dissolution of PVDF method with NMP solvent and the reference PVDF sample [7].

As can be seen from Figure 4.6, I_{003}/I_{104} of the non-pyrolysed cathode active materials is 1.712, indicating the non-pyrolysed cathode active materials show a characteristic layered structure. I_{003}/I_{104} of the cathode active materials reduces clearly following both pyrolysis experiments, explaining that cation mixing phenomena has occurred. Bearing in mind that neither carbothermal reaction nor self-decomposition at this level of temperatures is not possible, also PVDF is not entirely eliminated using dissolution of PVDF method, therefore, the TM degradation and cation mixing caused by the formation of HF, which affects the layered structure and particularly Li^{+1} ions, should be considered the primary causes of the reduction in I_{003}/I_{104}.

The layered structure of $Li(Ni_{1/3}Co_{1/3}Mn_{1/3})O_2$ was attacked by HF and also LiF formation was occurred so that transition metals might occupy (104) plane which leads cation mixing.

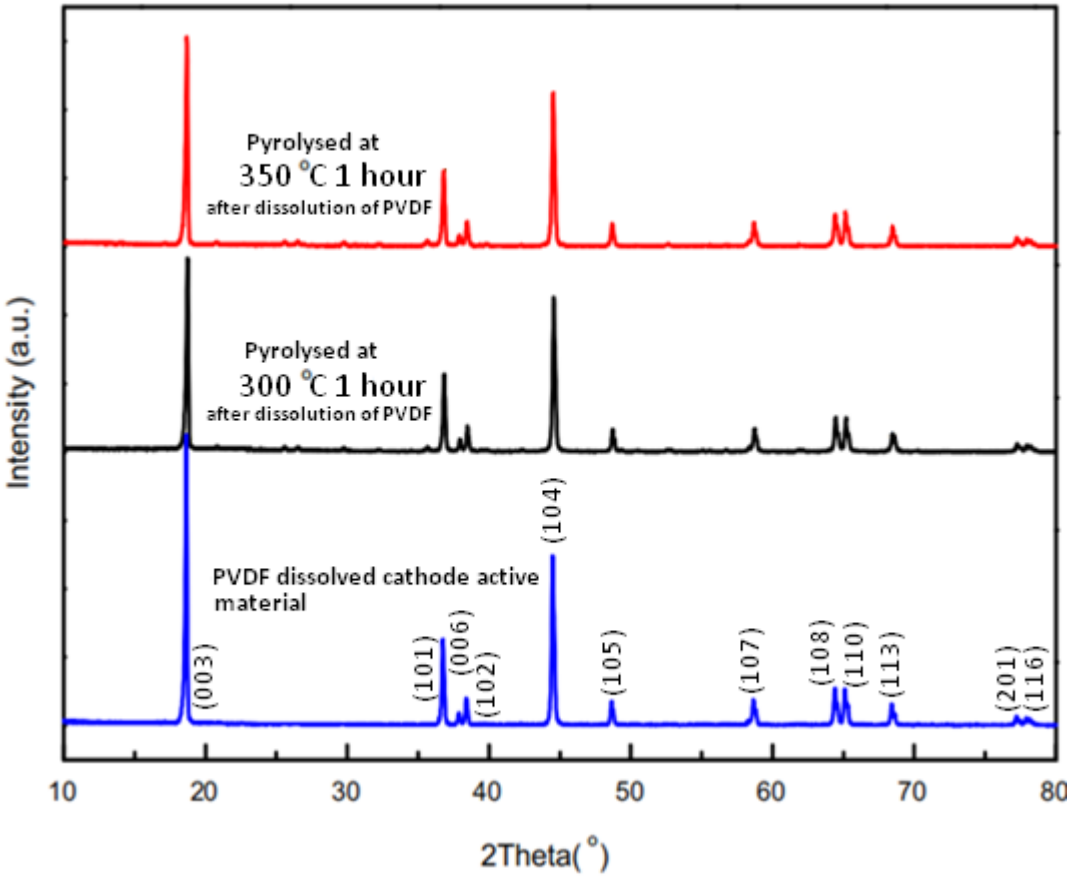

Figure 4.6. XRD patterns of the cathode active materials after dissolution of PVDF method that are pyrolysed at different temperatures.

From the SEM micrograph of the cathode active materials pyrolysed at distinct temperatures in Figure 4.7, in the non-pyrolysed cathode active materials, it is clear that $Li(Ni_{1/3}Co_{1/3}Mn_{1/3})O_2$ and carbon black have aggregated to some extent. This phenomena shows that PVDF was not completely eliminated before pyrolysis, that fits with the FTIR results shown in Figure 4.5. After pyrolysis at 300°C and 350°C, the agglomeration degree is reduced obviously, which may be related to the removal

of PVDF. In addition, the decomposition of some $Li(Ni_{1/3}Co_{1/3}Mn_{1/3})O_2$ because of HF from PVDF can also reduce the agglomeration degree.

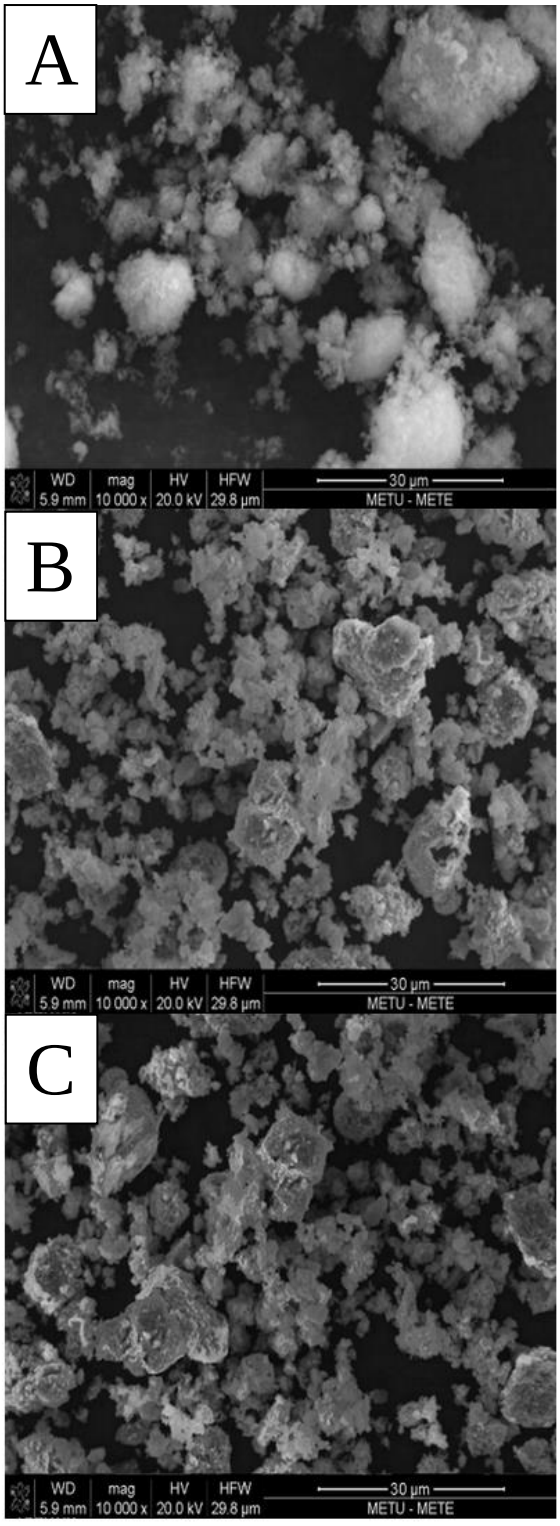

Figure 4.7. SEM micrographs of the cathode active materials pyrolysed at different temperatures (A) non-pyrolysed, (B) 300°C 1 h, and (C) 350°C 1 h.

Figure 4.8 displays the charge/discharge capacity behaviour of the cathode active materials pyrolysed at distinct temperatures. The non-pyrolysed cathode active materials have a discharging capacity of 145 $mAhg^{-1}$, that is comparable to the not used $Li(Ni_{1/3}Co_{1/3}Mn_{1/3})$ (155 $mAhg^{-1}$) and exhibits a strong capacity retention. Cathode active materials heated to 300 °C have a 144 $mAhg^{-1}$ discharge capacity, however its capacity retention is weak.

The maximum discharge capacity of pyrolysed cathode active materials at 350 °C was 109 $mAhg^{-1}$ is, a value much below that of not used cathode materials. As shown, residual PVDF has no negligible effect on the electrochemical performance of unheated cathode active materials, that exhibits the greatest electrochemical performance. Pyrolysis shows no positive contribution on the performance of cathode active materials in terms of neither capacity nor cycle life. The results are in line with the XRD patterns in Figure 4.6.

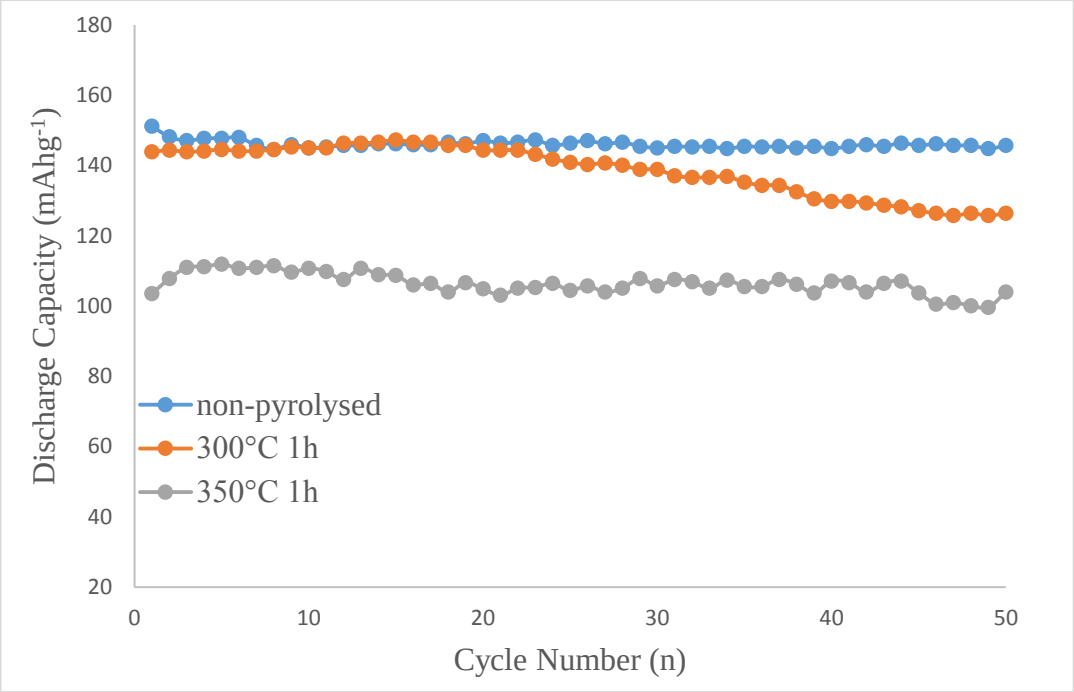

Figure 4.8. Cycle life of the cathode active materials that non-pyrolysed(specimen after dissolution of PVDF method), pyrolysed at 300°C and at 350°C temperatures.Besides structural, morphological, and electrochemical properties; particle diameters and the size distributions are essential factors for LIB cathode materials. Figure 4.9 demonstrates the particle size distribution graph of the cathode active materials pyrolysed at distinct temperatures.

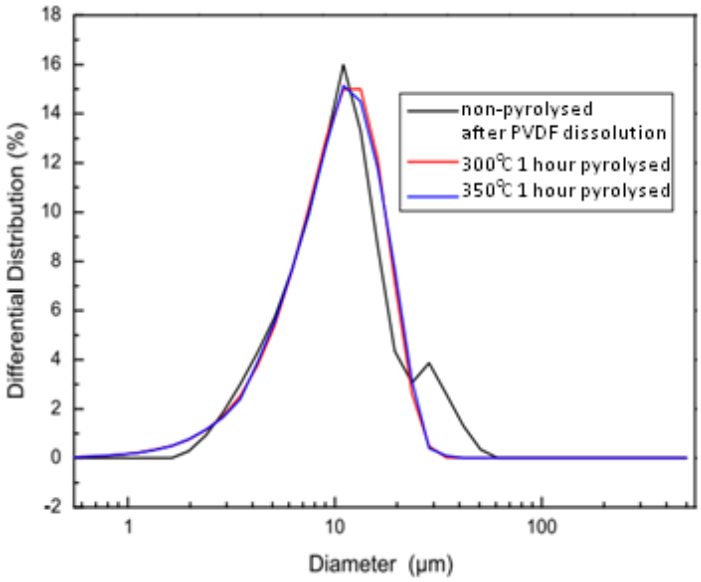

μm	D50	D10	D25	D75	D90
unheat-treated	9.48	4.17	6.37	13.14	21.03
300 °C 1 h	9.42	3.99	6.30	12.98	16.56
350 °C 1 h	9.39	3.97	6.27	12.87	16.20

Figure 4.9. The size distribution curve of the cathode active materials pyrolysed at different temperatures.

The particle size distribution graph in Figure 4.9. of the unheated cathode active materials shows a bimodal distribution model around 9 μm mostly and a little distribution peak on approximately 20 μm. The small distribution peak vanishes and the average particle diameter (D50) modestly lowers following pyrolysis at 300°C and 350°C. The little peak around 20 μm can be attributed to formation of agglomerates; following pyrolysis, the degree of agglomeration is decreased, therefore D_{50} lowers slightly. The explanation is the same as SEM in Figure 4.7.

4.2.3 Dissolution of Aluminum Method

After the 1 Molar NaOH solution reached 80°C, scissor-cut 1x1 cm^2 cathode plates were gradually added to the mixing solution.

The following reaction took place.

$$2Al_{(s)} + 2NaOH_{(aq)} + 2H_2O_{(l)} \rightarrow 2NaAlO_{2(aq)} + 3H_{2(g)}$$

As in the reaction, aluminum metal bonds with sodium in the basic media and turns into sodium aluminate, a compound with high water solubility. After mixing, the solution was filtered by vacuum filtration. The solid residues on the filter paper were washed 5 times with hot water and any remaining solutions were removed. After drying the solid, ICP-OES analysis was performed, as can be seen in Table 4.1.

Table 4.1 ICP-OES analysis of cathode active materials after 1 M NaOH Al dissolving method.

	Al ppm	Co ppm	Mn ppm	Ni ppm	Li ppm
Spent Cathode	52367	74481	88061	319580	60199
Filtrate Particles	28535	74626	88212	335525	45670
Mother Liquid	13212	0	0	1	13284
Washing Liquid	121	0	0	0	1245

Looking at the values shown in Table 4.1, the 1 M NaOH solution was insufficient to dissolve all the aluminum in the cathode plates. Filtrate particles which are cathode active materials still contain 2.8g/kg aluminum. This amount of aluminum is too much to produce cathodes by preparing sludge from these powders. For this reason, studies were also carried out with 2 M NaOH solution.

Table 4.2 ICP-OES analysis of cathode active materials after 2 M NaOH Al dissolving method.

	Al ppm	Co ppm	Mn ppm	Ni ppm	Li ppm
Spent Cathode	52367	74481	88061	319580	60199
Filtrate Particles	17387	74626	88212	335525	42101
Mother Liquid	31358	0	0	1	16252
Washing Liquid	121	0	0	0	874

In the repeated study with 2 M NaOH solution, the ICP-OES analysis results shown in Table 4.2 were obtained. As can be seen in this table, more aluminum was removed from the cathode active material compared to the 1 M NaOH solution. However, the filtrate particles still contain large amounts of aluminum. For this reason, studies were also carried out with 3 M NaOH solution.

Table 4.3 ICP-OES analysis of cathode active materials after3 M NaOH Al dissolving method.

	Al ppm	Co ppm	Mn ppm	Ni ppm	Li ppm
Spent Cathode	52367	74481	88061	319580	60199
Filtrate Particles	16450	74626	88212	335525	44721
Mother Liquid	33022	0	0	1	17320
Washing Liquid	421	0	0	0	762

As seen in Table 4.3, it is seen that increasing the concentration of the NaOH solution from 2 Molars to 3 Molars makes little or no difference. For this reason, it can be stated that it is not possible to remove aluminum pollution completely from the active material with the dissolution of aluminum method using NaOH. Also it is important to note that basic media dissolves lithium as well.

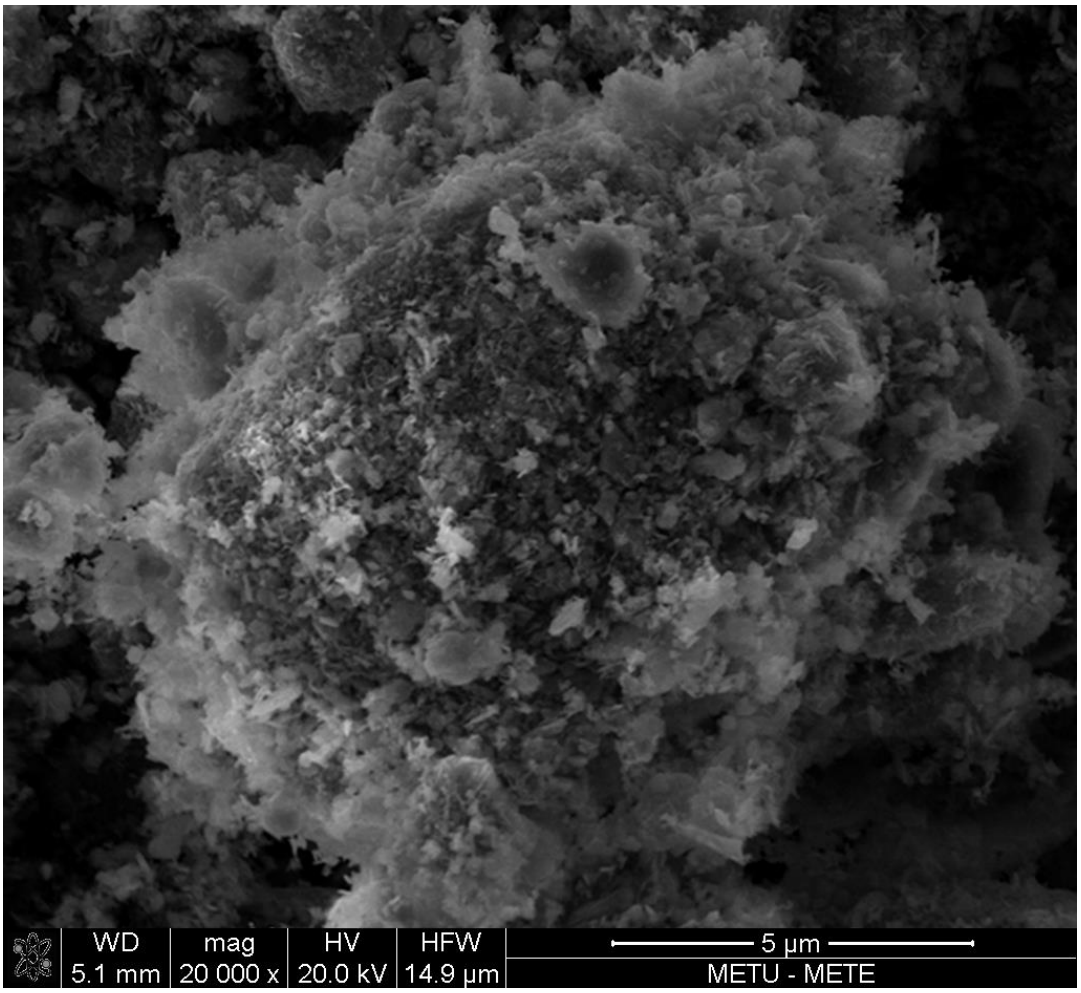

Figure 4.10. SEM image of the cathode active material which was obtained with 3 M NaOH Al dissolving method.

As can be seen from the Figure 4.10., particles of the cathode active material are both agglomerated and coarse. It shows that the inability of the alkali solution to reach all aluminum and dissolve the aluminum inside the particles.

To investigate the effect of retained aluminum on the cathode active materials on the electrochemical performance of the cathode active material, sludge was prepared from the obtained particles from 3 M NaOH dissolution reaction. Cycle capacity test was carried out by plastering the slurry on a new electrode. Test was carried with the current based on again referencing the capacity of NMC-111 cathode is 155 mAh/g at voltage window of 2.7 – 4.3V .

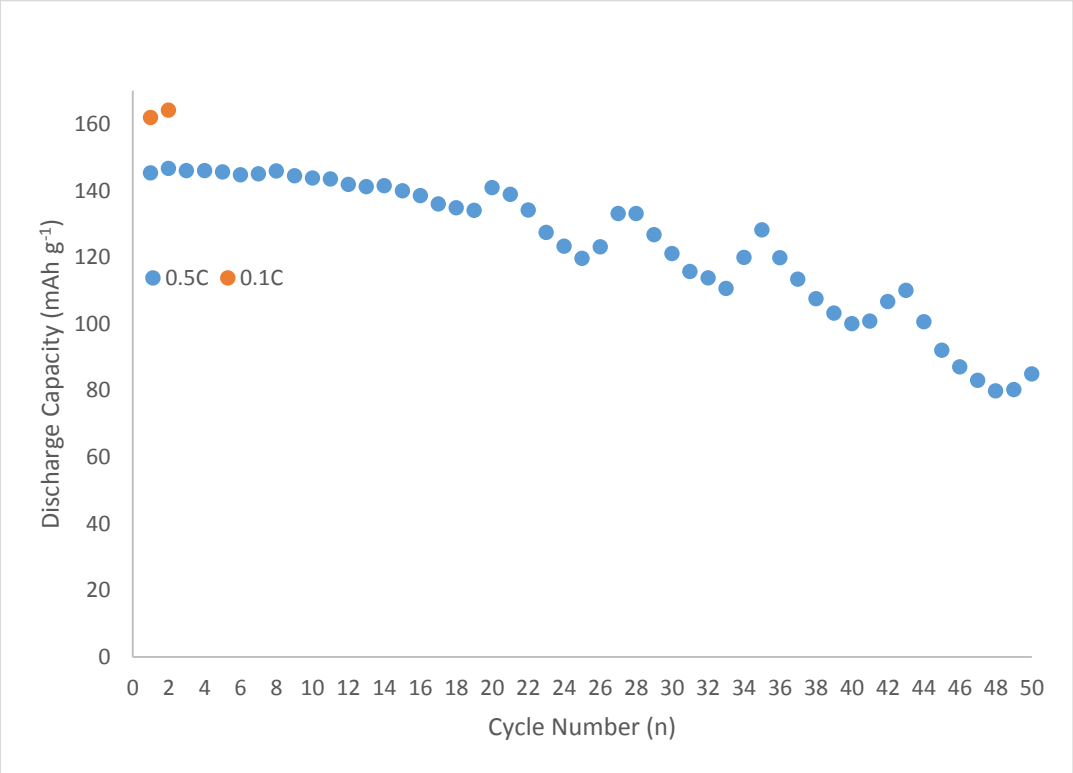

Figure 4.11. Cycle life of the $Li(Ni_{1/3}Co_{1/3}Mn_{1/3})O_2$ cathode active material which was obtained from Al dissolution method with 3 M NaOH solution.

As can be seen from Figure 4.11., the initial capacity of the cathode was acceptable for NMC-111 composition but the capacity retention of the cathode was extremely poor.

To conclude this method, it can not utilize for direct recycling of the spent cathodes because of the residual aluminum leads negative effects on the cathode active material properties. Instead, it can be used to pre-remove aluminum prior to acid leaching.

4.3 Method of Acid Leaching For Direct Co-precipitation With the Leachate Solution

Table 4.4. shows the leaching efficiency results derived from the performed ICP-OES analyses. In the first comparison experiment with 2 molar acids, it was seen that leaching with HCl acid is superior to other acids in terms of leaching efficiencies, up to 99% Li, 96% Ni and Co and 88% Mn by weight. Furthermore, 3 molar and 4 molar leaching experiments were also carried out with HCl acid and it was seen that 3 molar HCl acid results satisfying leaching efficiency. However, since the vapor pressure of the HCl acid solution is high, it is harmful to both environment and human health. In addition, HCl acid is much more corrosive than other acids due to the Cl^- ions it contains. When HNO_3 is used at 2 molars, Ni and Co leaching efficiencies are low, which are 84% and 81% by weight, respectively, but it can create a synergistic effect with H_2O_2 resulting in high leaching efficiencies.

H_2SO_4, on the other hand, shows a much higher synergistic effect with H_2O_2. For this reason, leaching studies were carried out with 3 molar H_2SO_4 with 5 vol% and 10 vol% H_2O_2. It was shown that the highest leaching efficiency when used as 4 molars, moreover, when 10 vol% H_2O_2 is added. By this way, 99% Li, 98% Ni, 97% Co and 95% Mn by weight recovery efficiencies were achieved.

H_3PO_4 is insufficient in leaching efficiency compared to other acids.

Among these three acids, H_2SO_4 was chosen because of its availability, having lower vapor pressure than HCl, cost efficiency and showing highly synergetic effects with both reducing reagents. Another advantage of this acid is that sulfate ions will not

cause any problem when the co-precipitation stage is started with the pregnant leach solution. Chloride ions or nitride ions can cause pre-precipitation problems at the co-precipitation stage.

Inorganic acids were compared to determine which acid is feasible to use in the leaching stage. In this step, all other parameters were set to constant values. HCl was strong enough to leach the substrate even used in 2 molars however this acid leads to containment and environmental problems as its low vaporization temperature and very aggressive in terms of corrosion problems. HNO_3 works in 4 molars and uses H_2O_2 as a reducing agent to leach effectively but H2SO4 is a cheaper and more available acid, so H_2SO_4 concentration was determined after. H_2SO_4 acid and H_2O_2 as reducing agent works very synergistically.

After deciding on the concentrations of the acid and reductant couple, the temperature parameter was examined. In fact, in acid leaching studies, the leaching efficiency increases as the temperature is increased, so leaching was carried out at 80°C until this stage in terms of safe operation under atmospheric conditions. It was observed whether there was a large difference in leaching efficiency by lowering the temperature. While there is a negligible difference at 70°C when compared to 80°C, efficiency decreases as the temperature decreases.

The mixing time parameter, on the other hand, is expected to show a direct proportion as in the temperature parameter. When the mixing time is reduced from 3 hours to 2 hours and 1 hour, a decrease in leaching efficiency is observed.

After that, SO_2 gas, an alternative reducing agent was studied with 4M H_2SO_4 solution. Piping 0.5 lt/min SO_2 gas into agitating media was enough to reduce most of the metals. Leaching efficiency when using SO_2 is very close to using H_2O_2 solution, which are up to 99% Li, 98% Ni, 97% Co and 95% Mn by weight.

In summary, using 4 molars H_2SO_4 as an acid and 10 Vol% H_2O_2 or 0.5 l/min SO_2 gas as the reducing agent at the 80°C temperature and 3 h of agitation under a

mechanical mixer coated with PTFE and 280 RPM were determined to be the most feasible approach in terms of leaching efficiency, cost and suitability for co-precipitation method.

Table 4.4 Acid leaching experiments and leach efficiencies.

No	Leaching Treatment			Leach Temp (◦C)	Time(h)	Leach Efficiency (%)			
A	**Inorganic Leaching Agent**		**Reducing Agent**			Li	Ni	Co	Mn
1	HCl	4 mol L-1	N/A	80	3	99	96	96	88
2	HCl	3 mol L-1	N/A	80	3	99	95	96	88
3	HCl	2 mol L-1	N/A	80	3	98	87	88	83
4	HNO_3	2 mol L-1	N/A	80	3	96	84	81	80
5	HNO_3	2 mol L-1	H_2O_2 (5 Vol%)	80	3	98	87	88	90
6	HNO_3	3 mol L-1	H_2O_2 (5 Vol%)	80	3	98	89	87	91
7	HNO_3	4 mol L-1	H_2O_2 (5 Vol%)	80	3	99	88	90	93
8	H_2SO_4	1 mol L-1	N/A	80	3	82	75	72	68
9	H_2SO_4	2 mol L-1	N/A	80	3	96	85	83	74
10	H_2SO_4	3 mol L-1	N/A	80	3	97	86	87	76
11	H_2SO_4	3 mol L-1	H_2O_2 (5 Vol%)	80	3	98	94	95	92
12	H_2SO_4	3 mol L-1	H_2O_2 (10 Vol%)	80	3	99	97	96	94
13	H_2SO_4	4 mol L-1	N/A	80	3	97	87	88	75
14	H_2SO_4	4 mol L-1	H_2O_2 (10 Vol%)	80	3	99	98	97	95
15	H_2SO_4	4 mol L-1	SO_2	80	3	99	97	96	98
16	H_3PO_4	2 mol L-1	N/A	80	3	93	81	80	75
17	H_3PO_4	2 mol L-1	H_2O_2 (10 Vol%)	80	3	97	88	85	82
18	H_2SO_4	4 mol L-1	H_2O_2 (10 Vol%)	80	3	99	98	97	95
19	H_2SO_4	4 mol L-1	H_2O_2 (10 Vol%)	70	3	99	97	96	95
20	H_2SO_4	4 mol L-1	H_2O_2 (10 Vol%)	60	3	98	94	95	92
21	H_2SO_4	4 mol L-1	H_2O_2 (10 Vol%)	25	3	87	73	70	75
22	H_2SO_4	4 mol L-1	H_2O_2 (10 Vol%)	80	3	99	98	97	95
23	H_2SO_4	4 mol L-1	H_2O_2 (10 Vol%)	80	2	99	96	95	88
24	H_2SO_4	4 mol L-1	H_2O_2 (10 Vol%)	80	1	97	83	85	78

4.3.1 Adjusting and Direct Cathode Active Material Synthesis Method

Pregnant leach solution comprising Li, Ni, Co, and Mn was characterized by ICP-OES and the results are shown in Table 4.5.

Table 4.5 ICP-OES result of the pregnant leach solution obtained from acid leaching stage.

Li ppm	Ni ppm	Mn ppm	Co ppm
4172	24303	6165	5598

So stoichiometrical calculations were made batchwisely. 24.30 g/L Ni, 6.16 g/L Mn, and 5.60 g/L Co in PLS were determined. These masses divided by the atomic weights of Ni, Co and Mn ,respectively, give the moles. Then mole fractions were calculated and in this batch was NMC 0.67:0.18:0.15. This cathode chemistry is near to well-known NMC622, so that adding manganese sulfate and cobalt sulfate into the PLS in an appropriate stoichiometrical amount to achieve NMC622 was done.

After that, with this solution, the co-precipitation method is applied to co-precipitate $Ni_{0.6}Mn_{0.2}Co_{0.2}(OH)_2$. As can be seen from Figure 4.12, the capacity retention of the cell is 94.2% after 50 cycles at 0.5C charge/discharge rate. The first capacity of the re-synthesized cell is 151.58 $mAhg^{-1}$ and at 50^{th} cycle is 142.83 $mAhg^{-1}$ with 0.5C charge/discharge rates. The SEM micrograph in Figure 4.13 shows that the particles are round-shaped and between 8-10 μm. The spherical morphology of these particles provides a better coating to aluminum so that commercial cathode active material particles are spherical. The XRD pattern of the synthesized active material powders is shown in Figure 4.14. All peaks of the characteristics of layered NMC cathode structure can be seen clearly.

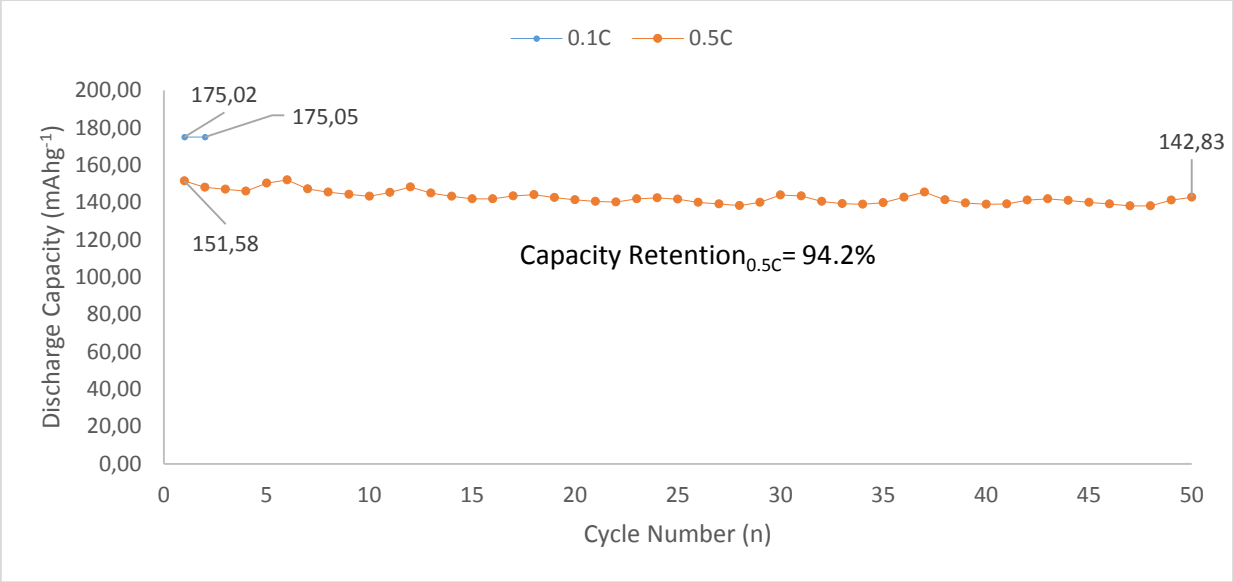

Figure 4.12. Cycle life of the $Li(Ni_{0.6}Mn_{0.2}Co_{0.2})O_2$ cathode active material synthesized using acid leach solution.

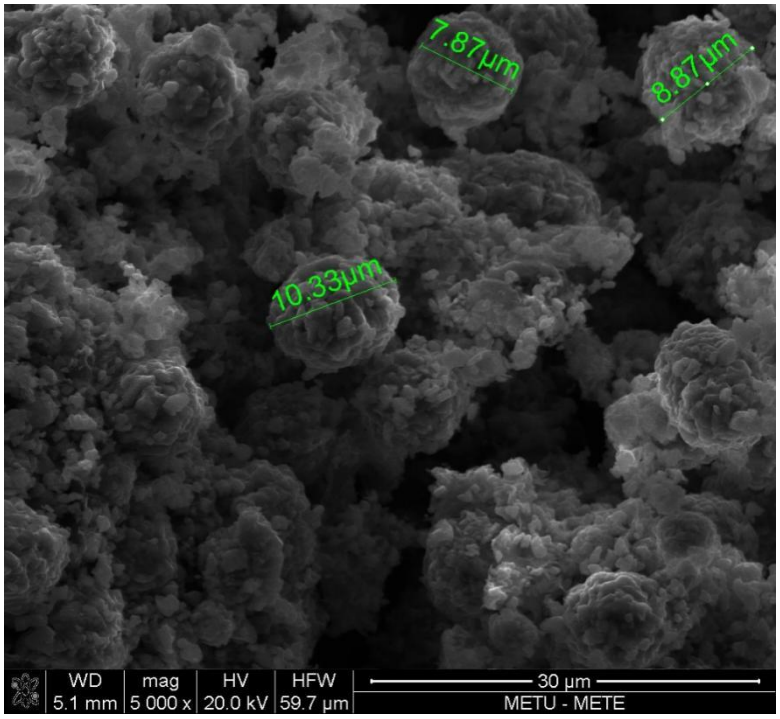

Figure 4.13. SEM micrograph of synthesized $Li(Ni_{0.6}Mn_{0.2}Co_{0.2})O_2$ particles synthesized using acid leach solution.

In Figure 4.14., the XRD pattern of the synthesized cathode active material is shown. All of the characteristic peaks of the layered structure can be clearly identified. Co-precipitation method seems succesful for the acid leach solution of spent LIBs and neither any impurities nor the unexpected phase formation are not present in the synthesized material.

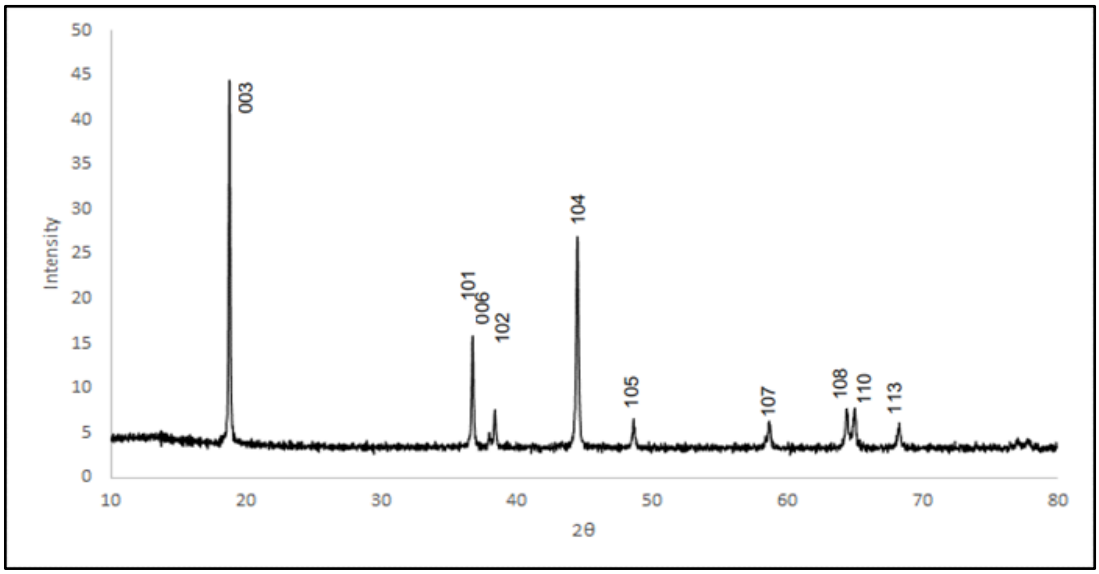

Figure 4.14. XRD pattern of re-synthesized $Li(Ni_{0.6}Mn_{0.2}Co_{0.2})O_2$.

CHAPTER 5

CONCLUSIONS

The aim of this study was to investigate a process to recover the material from the cathodes of waste lithium-ion batteries through closed-loop recycling processes and to produce electrodes from them again.

For this purpose, two different approaches were studied. The first approach was to strip the materials off the aluminum foil at the cathode. Three different methods were used for this. Pyrolysis method, dissolution of PVDF method and dissolution of aluminum foil method.

The pyrolysis method aimed to remove the binder PVDF by decomposing it. However, PVDF, which decomposes with the increase in temperature, released HF gas. None the less, it was observed that HF caused structural changes by destroying the cathode active material in the environment.

In the dissolution PVDF method, the aim was to dissolve the binder PVDF using NMP. As there was no binder left between the cathode active material and the aluminum foil due to the PVDF being dissolved, the active material was separated from the foil. However, the undissolved PVDF remained in the particles and could not be completely removed, causing an agglomeration in the active material. Although capacity retention and discharge capacity are high in electrochemical tests, it is not desired because agglomeration creates problems during sludge preparation and plastering on the foil.

The aluminum foil dissolving method, on the other hand, aims to dissolve the aluminum, which is the current collector, to release the active material on it. In this method, it was observed that the aluminum foil could not be completely removed

and there was always remained aluminum detected between the particles. When the cathode active materials obtained by this method are prepared as sludge and electrochemical tests are performed, it has been determined that it causes a very serious decrease on the capacity retention.

In the second approach, it was aimed to recover the lithium, nickel, cobalt and manganese from the waste cathodes into solution by acid leaching and then to synthesize the cathode active material precursor by direct co-precipitation method with this solution. Strong inorganic acids and reducing agents were used for the leaching process. Leaching yields were very close to 100% w/w for these metals. Aluminum was also dissolved, but was subsequently removed from the solution by alkali precipitation. Ni, Co and Mn in the solution were precipitated in a layered structure, which is the desired crystal lattice, by the co-precipitation method and electrochemical tests were carried out after calcination processes. It gave the identical layered structure perfectly in XRD analyzes, and gave satisfactory high values in terms of capacity retention and discharge capacity values in electrochemical tests.

It is observed that the most reliable method for the closed-circuit recycling of waste lithium-ion batteries is to set up a leaching process as in the second approach. Afterwards, it is possible to synthesize the cathode active material again with the obtained solution. Moreover, it has been proven that there is no need for unnecessary and costly steps, such as obtaining individual salts of all metals with high purity, and then preparing solutions with these salts and synthesizing active material, as is the case with conventional methods.

REFERENCES

1. Dawei Song, Xiaoqing Wang, Enlou Zhou, Peiyu Hou, Fenxia Guo, Lianqi Zhang. "Recovery and heat treatment of the Li(Ni1/3Co1/3Mn1/3)O2 cathode scrap material for lithium ion battery", Journal of Power Sources, 2013

2. Tyler Or, Storm W. D. Gourley, Karthikeyan Kaliyappan, Aiping Yu, Zhongwei Chen. "Recycling of mixed cathode lithium- ion batteries for electric vehicles: Current status and future outlook", Carbon Energy, 2020

3. Kunhong Gu, Jiahui Chang, Xiaohui Mao, Hongbo Zeng, Wenqing Qin, Junwei Han. "Efficient separation of cathode materials and Al foils from spent lithium batteries with glycerol heating: A green and unconventional way", Journal of Cleaner Production, 2022

4. Wen Xuan, Antônio Braga de Souza, Chloé Korbel, Alexandre Chagnes. "New insights in the leaching kinetics of cathodic materials in acidic chloride media for lithium-ion battery recycling", Hydrometallurgy, 2021

5. Wen Xuan, Antônio de Souza Braga, Alexandre Chagnes. "Development of a Novel Solvent Extraction Process to Recover Cobalt, Nickel, Manganese, and Lithium from Cathodic Materials of Spent Lithium-Ion Batteries", ACS Sustainable Chemistry & Engineering, 2021

6. Dawei Song, Xiaoqing Wang, Hehe Nie, Hua Shi, Dongge Wang, Fenxia Guo, Xixi Shi, Lianqi Zhang. "Heat treatment of LiCoO2 recovered from cathode scraps with solvent method", Journal of Power Sources, 2014

7. G. J. Wang. "An aqueous rechargeable lithium battery based on LiV3O8 and Li[Ni1/3Co1/3Mn1/3]O2", Journal of Applied Electrochemistry, 04/2008

8. Ferreira, S.L.C.. "The determination of molybdenum in water and biological samples by graphite furnace atomic spectrometry after polyurethane foam column separation and preconcentration", Talanta, 20031223

9. Kirti Richa, Callie W. Babbitt, Gabrielle Gaustad, Xue Wang. "A future perspective on lithium-ion battery waste flows from electric vehicles", Resources, Conservation and Recycling, 2014

10. Şerife Tokalıoğlu, Şenol Kartal, Latif Elçi. "Determination of heavy metals and their speciation in lake sediments by flame atomic absorption spectrometry after a four-stage sequential extraction procedure", Analytica Chimica Acta, 2000

11. Ying Zheng, Shiquan Wang, Yinglong Gao, Tao Yang, Qinwen Zhou, Wei Song, Chen Zeng, Huimin Wu, Chuanqi Feng, Jianwen Liu. "Lithium Nickel Cobalt Manganese Oxide Recovery via Spray Pyrolysis Directly from the Leachate of Spent Cathode Scraps", ACS Applied Energy Materials, 2019

12. Duygu Karabelli, Steffen Kiemel, Soumya Singh, Jan Koller, Simone Ehrenberger, Robert Miehe, Max Weeber, Kai Peter Birke. "Tackling xEV Battery Chemistry in View of Raw Material Supply Shortfalls", Frontiers in Energy Research, 2020

13. Zhilin Liang, Chen Cai, Gangwei Peng, Jingping Hu, Huijie Hou, Bingchuan Liu, Sha Liang, Keke Xiao, Shushan Yuan, Jiakuan Yang. "Hydrometallurgical Recovery of Spent Lithium Ion Batteries: Environmental Strategies and Sustainability Evaluation", ACS Sustainable Chemistry & Engineering, 2021

14. Junmin Nan, Dongmei Han, Minjie Yang, Ming Cui, Xianlu Hou. "Recovery of metal values from a mixture of spent lithium-ion batteries and nickel-metal hydride batteries", Hydrometallurgy, 2006

15. Shi Chen, Yu Zheng, Yun Lu, Yuefeng Su, Liying Bao, Ning Li, Yitong Li, Jing Wang, Renjie Chen, Feng Wu. "Enhanced Electrochemical Performance of Layered Lithium-Rich Cathode Materials by Constructing Spinel-Structure Skin and Ferric Oxide Islands", ACS Applied Materials & Interfaces, 2017

16. Md Ishtiaq Hossain Khan, Masud Rana, Theoneste Nshizirungu, Young Tae Jo, Jeong- Hun Park. "Recovery of Valuable and Hazardous Metals (Ni, Co, and Cd) from Spent Ni–Cd Batteries Using Polyvinyl Chloride (PVC) in Subcritical Water", ACS Sustainable Chemistry & Engineering, 2022

17. Xiangqi Meng, Hongbin Cao, Jie Hao, Pengge Ning, Gaojie Xu, Zhi Sun. " Sustainable Preparation of LiNi Co Mn O –V O Cathode Materials by Recycling Waste Materials of Spent Lithium-Ion Battery and Vanadium-Bearing Slag ", ACS Sustainable Chemistry & Engineering, 2018

18. S. Agatzini-Leonardou, P.E. Tsakiridis, P. Oustadakis, T. Karidakis, A. Katsiapi. "Hydrometallurgical process for the separation and recovery of nickel from sulphate heap leach liquor of nickeliferrous laterite ores", Minerals Engineering, 2009

19. Weng, Yaqing, Shengming Xu, Guoyong Huang, and Changyin Jiang. "Synthesis and performance of Li[(Ni1/3Co1/3Mn1/3)1−xMgx]O2 prepared from spent lithium ion batteries", Journal of Hazardous Materials, 2013.

20. Hiroshi Okano, Yuta Hano, Kaito Sugimoto, Fumiya Ohira et al. "Lead acid battery with high resistance to over- discharge using graphite based materials as cathode current collector", Nano Select, 2021

21. Yiguan Lu, C. Michael Lesher, Jun Deng. "Geochemistry and genesis of magmatic Ni- Cu-(PGE) and PGE-(Cu)-(Ni) deposits in China", Ore Geology Reviews, 2019

22. Amilton Barbosa Botelho Junior, Srecko Stopic, Bernd Friedrich, Jorge Alberto Soares Tenório, Denise Crocce Romano Espinosa. "Cobalt Recovery from Li-Ion Battery Recycling: A Critical Review", Metals, 2021

23. Hou, Peiyu, Xiaoqing Wang, Dawei Song, Xixi Shi, Jian Guo, Jun Zhang, and Lianqi Zhang. "Design, preparation and properties of core- shelled Li{[NiyCo1-2yMny](1- x)}core{[Ni1/2Mn1/2]x}shellO2 (0≤x≤0.3, 6y+3x-6xy=2) as high-performance cathode for Li-ion battery", Electrochimica Acta, 2014.

24. Xuehua He, Zheng Li, Yuankui Wang, Wanli Xu et al. "A high-purity AgO cathode active material for high-performance aqueous AgO– Al batteries", Journal of Power Sources, 2022

25. Yating Du, Kosuke Fujita, Sayoko Shironita, Yoshitsugu Sone, Eiji Hosono, Daisuke Asakura, Minoru Umeda. "Capacity fade characteristics of nickel-based lithium-ion secondary battery after calendar deterioration at 80°C", Journal of Power Sources, 2021

26. "Recycling of Lithium-Ion Batteries", Springer Science and Business Media LLC, 2018

27. Ersha Fan, Li Li, Zhenpo Wang, Jiao Lin, Yongxin Huang, Ying Yao, Renjie Chen, Feng Wu. "Sustainable Recycling Technology for Li- Ion Batteries and Beyond: Challenges and Future Prospects", Chemical Reviews, 2020

28. Heesuk Ku, Yeojin Jung, Minsang Jo, Sanghyuk Park et al. "Recycling of spent lithium-ion battery cathode materials by ammoniacal leaching", Journal of Hazardous Materials, 2016

29. Jonas Neumann, Martina Petranikova, Marcel Meeus, Jorge D. Gamarra, Reza Younesi, Martin Winter, Sascha Nowak. "Recycling of Lithium- Ion

Batteries—Current State of the Art, Circular Economy, and Next Generation Recycling", Advanced Energy Materials, 2022

30. Kishore K. Jena, Akram AlFantazi, Ahmad T. Mayyas. "Comprehensive Review on Concept and Recycling Evolution of Lithium-Ion Batteries (LIBs)", Energy & Fuels, 2021

31. Minsang Jo, Heesuk Ku, Sanghyuk Park, Junho Song, Kyungjung Kwon. "Effects of Residual Lithium in the precursors of Li[Ni 1/3 Co 1/3 Mn 1/3]O 2 on their lithium-ion battery performance", Journal of Physics and Chemistry of Solids, 2018

32. Xiaoxiao Zhang, Qing Xue, Li Li, Ersha Fan, Feng Wu, Renjie Chen. "Sustainable Recycling and Regeneration of Cathode Scraps from Industrial Production of Lithium-Ion Batteries", ACS Sustainable Chemistry & Engineering, 2016

33. Yafei Jie, Shenghai Yang, Yun Li, Fang Hu, Duoqiang Zhao, Di Chang, Yanqing Lai, Yongming Chen. " Waste Organic Compounds Thermal Treatment and Valuable Cathode Materials Recovery from Spent LiFePO Batteries by Vacuum Pyrolysis ", ACS Sustainable Chemistry & Engineering, 2020

34. Yonglin Yao, Meiying Zhu, Zhuo Zhao, Bihai Tong, Youqi Fan, Zhongsheng Hua. "Hydrometallurgical Processes for Recycling Spent Lithium-Ion Batteries: A Critical Review", ACS Sustainable Chemistry & Engineering, 2018

35. Li, Haikun, Lindsay M. Corneal, and Charles R. Standridge. "Effects of acid concentration, temperature, and time on recycling of post- vehicle-application lithium-ion batteries of varying chemistries", Materials for Renewable and Sustainable Energy, 2015